



More Stories about CLFV

Yoshitaka Kuno
Department of Physics,
Osaka University, Japan

June 6th, 2019
cLFV School, IHEP, Beijing, China

Search for
New Physics



The Standard Model

Three Generations of Matter (Fermions)

	I	II	III		
mass →	2.4 MeV/c ²	1.27 GeV/c ²	171.2 GeV/c ²	0	125.9 GeV
charge →	2/3	2/3	2/3	0	0
spin →	1/2	1/2	1/2	1	0
name →	u up	c charm	t top	γ photon	H Higgs Boson
				0	
	4.8 MeV/c ²	104 MeV/c ²	4.2 GeV/c ²	0	
	-1/3	-1/3	-1/3	0	
	1/2	1/2	1/2	1	
Quarks	d down	s strange	b bottom	g gluon	
	<2.2 eV/c ²	<0.17 MeV/c ²	<15.5 MeV/c ²	91.2 GeV/c ²	
	0	0	0	0	
	1/2	1/2	1/2	1	
	ν_e electron neutrino	ν_μ muon neutrino	ν_τ tau neutrino	Z⁰ Z boson	
	0.511 MeV/c ²	105.7 MeV/c ²	1.777 GeV/c ²	80.4 GeV/c ²	
	-1	-1	-1	±1	
	1/2	1/2	1/2	1	
Leptons	e electron	μ muon	τ tau	W[±] W boson	
					Gauge Bosons

The Standard Model is considered to be incomplete.

ex.
mass and mixing,
strong CP,
dark matter,
baryogenesis,
dark energy

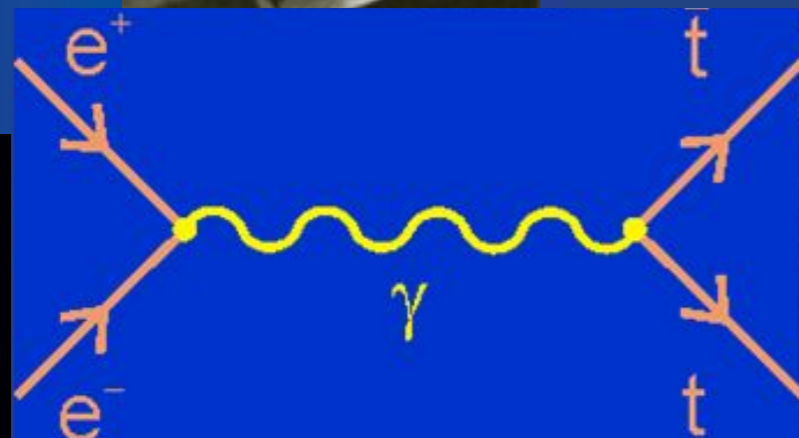
New Physics is needed.

High Energy Frontier and High Intensity Frontier

High Energy Frontier

$$E=mc^2$$

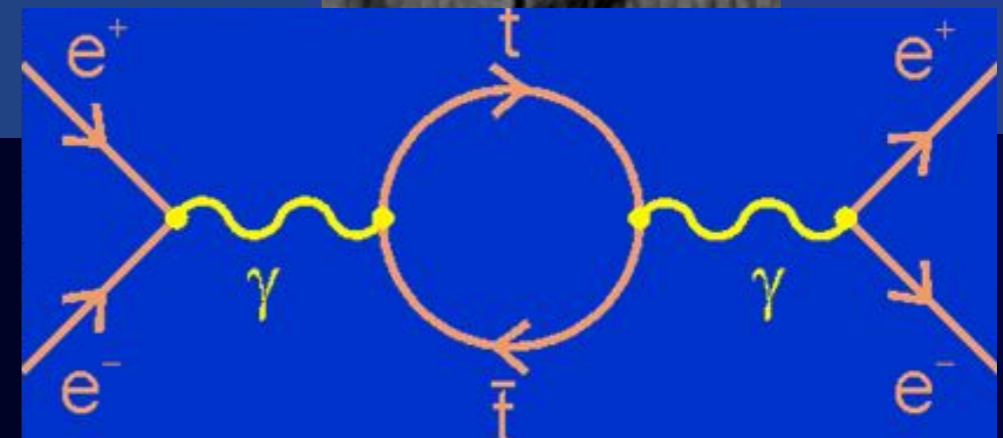
appearance of **real**
new particles



High Intensity Frontier

$$\Delta E \Delta t \gtrsim \hbar$$

appearance of **virtual**
new particles



Flavour Transitions

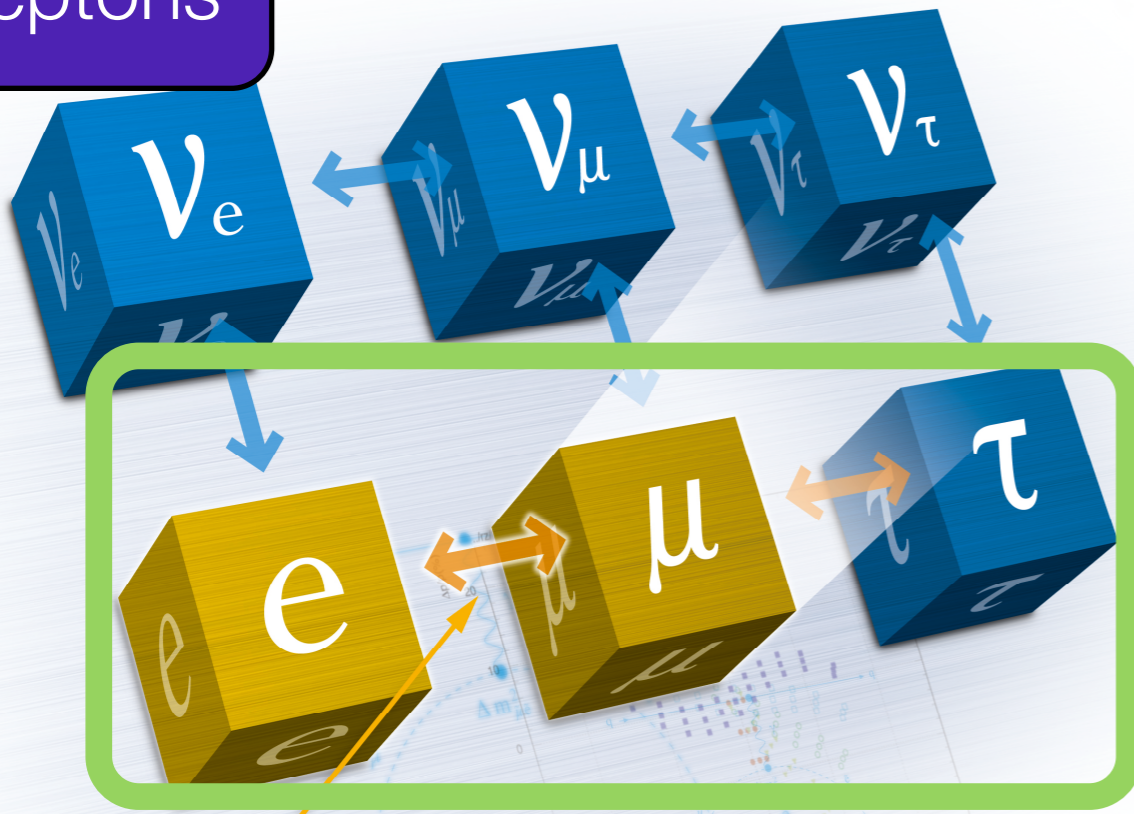
Quarks



Quark transition observed



Leptons



Neutrino transition observed

Charged lepton transition not observed.



New Physics Energy Scale of CLFV Search

Effective Field Theory (EFT) Approach

$$\mathcal{L}_{eff} = \mathcal{L}_{SM} + \sum_{d>4} \frac{C^{(d)}}{\Lambda^{d-4}}$$

Λ is the energy scale of new physics
 $C^{(d)}$ is the coupling constant.

from $BR(\mu \rightarrow e\gamma) < 4.2 \times 10^{-13}$

$$\frac{C^6}{\Lambda^2} \mathcal{O}^6 \rightarrow \frac{C^6}{\Lambda^2} \bar{e}_L \sigma^{\rho\nu} \mu_R \Phi F_{\rho\nu}$$



$$\Lambda \sim \mathcal{O}(10^4) \text{ TeV}$$

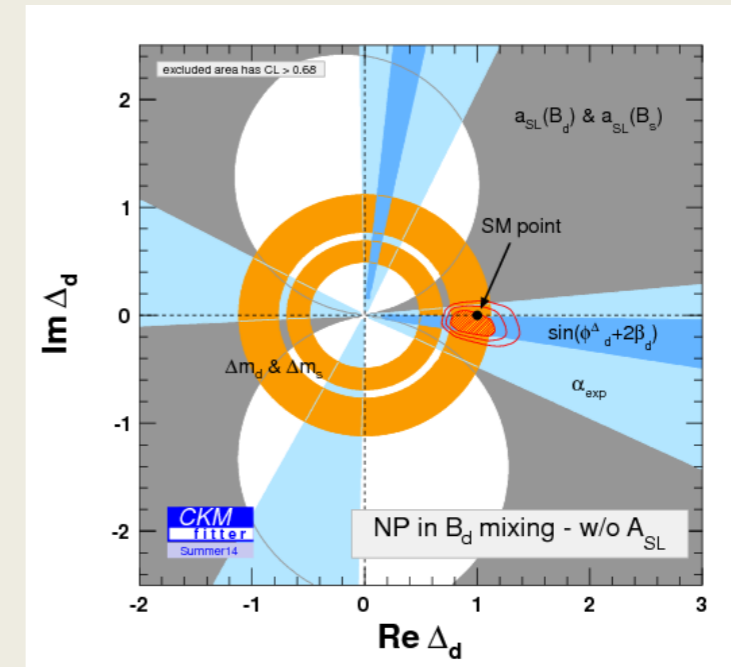
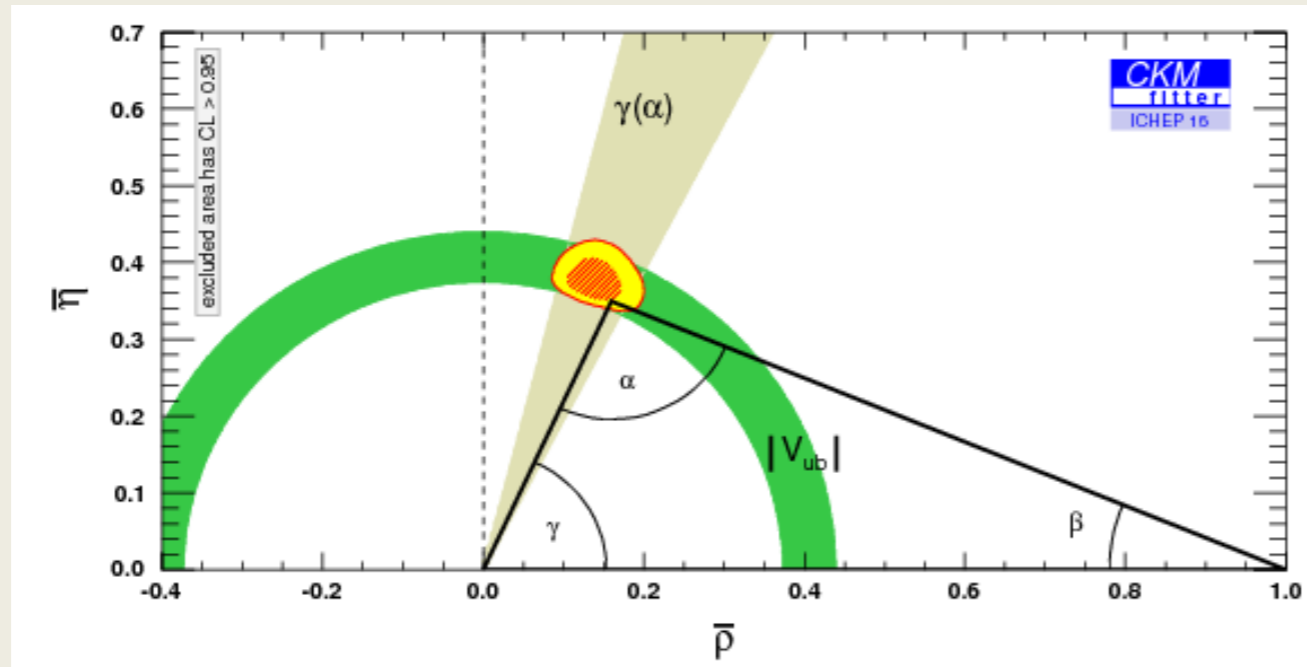
cf. : ϵ_K

	$ C_a [\Lambda = 1 \text{ TeV}]$	$\Lambda \text{ (TeV)} [C_a = 1]$	CLFV Process
$C_{e\gamma}^{\mu e}$	2.1×10^{-10}	<u>6.8×10^4</u>	$\mu \rightarrow e\gamma$
$C_{le}^{\mu\mu e, e\mu\mu}$	1.8×10^{-4}	75	$\mu \rightarrow e\gamma$ [1-loop]
$C_{le}^{\mu\tau\tau e, e\tau\tau\mu}$	1.0×10^{-5}	312	$\mu \rightarrow e\gamma$ [1-loop]
$C_{e\gamma}^{\mu e}$	4.0×10^{-9}	<u>1.6×10^4</u>	$\mu \rightarrow eee$
$C_{ll,ee}^{\mu eee}$	2.3×10^{-5}	207	$\mu \rightarrow eee$
$C_{le}^{\mu eee, ee\mu e}$	3.3×10^{-5}	174	$\mu \rightarrow eee$
$C_{e\gamma}^{\mu e}$	5.2×10^{-9}	<u>1.4×10^4</u>	$\mu^- \text{ Au} \rightarrow e^- \text{ Au}$
$C_{lq,ld,ed}^{e\mu}$	1.8×10^{-6}	745	$\mu^- \text{ Au} \rightarrow e^- \text{ Au}$
$C_{eq}^{e\mu}$	9.2×10^{-7}	1.0×10^3	$\mu^- \text{ Au} \rightarrow e^- \text{ Au}$
$C_{lu,eu}^{e\mu}$	2.0×10^{-6}	707	$\mu^- \text{ Au} \rightarrow e^- \text{ Au}$

F. Feruglio, P. Paradisi and A. Pattori, Eur. Phys. J. C 75 (2015) no.12, 579

G. M. Pruna and A. Signer, JHEP 1410 (2014) 014

Probing NP with FCNC



ij	Λ [TeV] CPC	Λ [TeV] CPV	Observables
sd	9.8×10^2	1.6×10^4	$\Delta m_K; \epsilon_K$
bd	6.6×10^2	9.3×10^2	$\Delta m_B; S_{\psi K}$
bs	1.4×10^2	2.5×10^2	$\Delta m_{B_s}; S_{\psi\phi}$

Lower bounds on the NP scale in $\frac{1}{\Lambda^2} (\bar{q}_{Li} \gamma_\mu q_{Lj})(\bar{q}_{Li} \gamma^\mu q_{Lj})$

New Physics Energy Scale of CLFV Search Future



Future planned experiments expecting improvements by an additional factor of $>10,000$ or more (will be described later) would probe

$$\Lambda \sim \mathcal{O}(10^5) \text{ TeV}$$

$$R \propto \frac{1}{\Lambda^4}$$

1

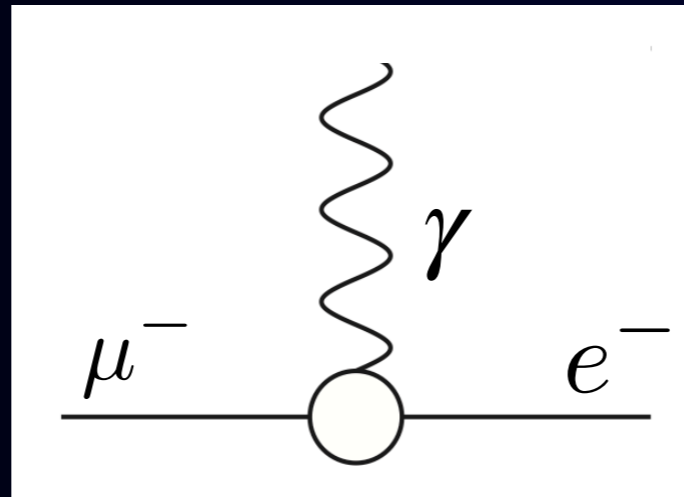
CLFV would explore scales way beyond the energies that our present and future colliders can directly reach.

It is crucial in establishing where is the next fundamental scale above the electroweak symmetry breaking.

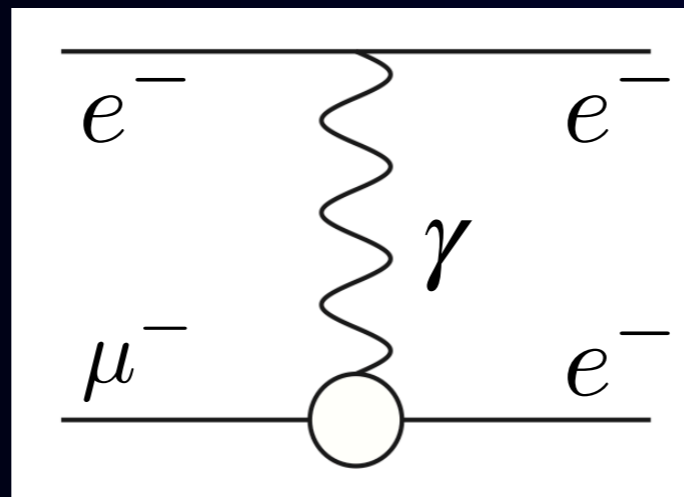
“Golden” $\mu \rightarrow e$ CLFV Transition Processes

dipole interaction

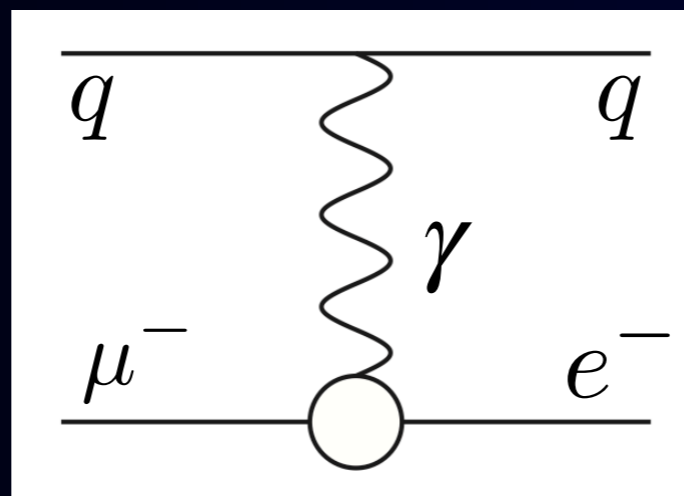
$$\mu^+ \rightarrow e^+ \gamma$$



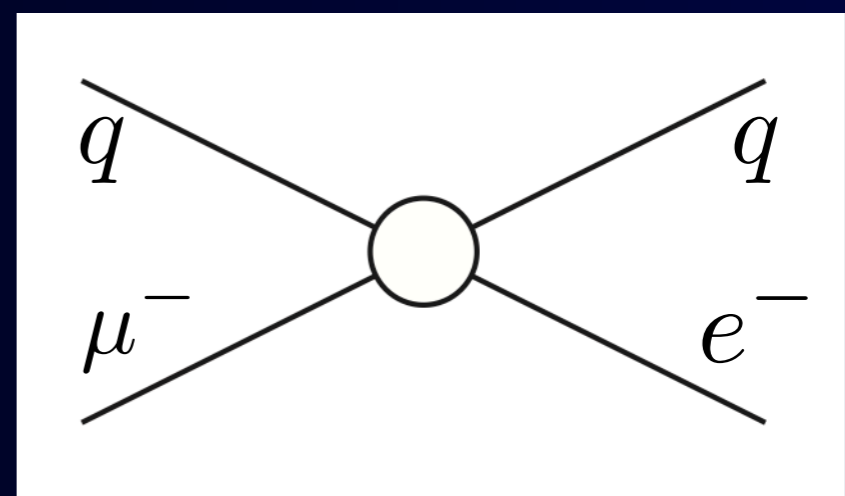
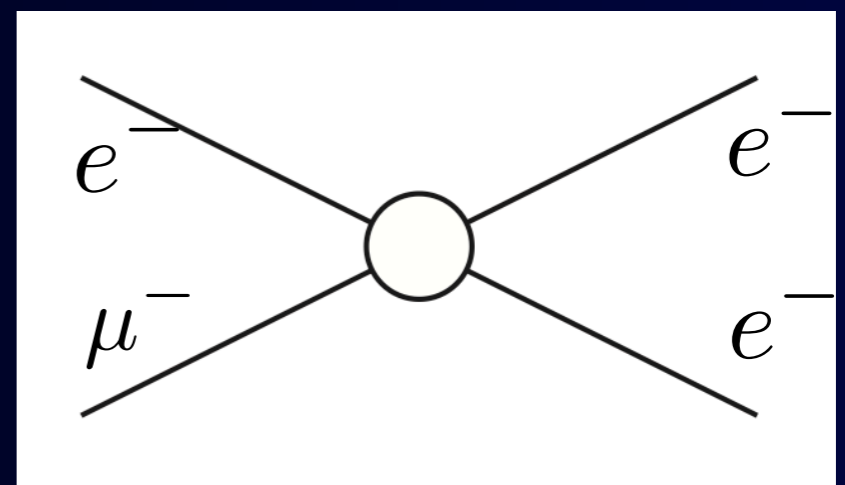
$$\mu^+ \rightarrow e^+ e^+ e^-$$



$$\mu^- N \rightarrow e^- N$$



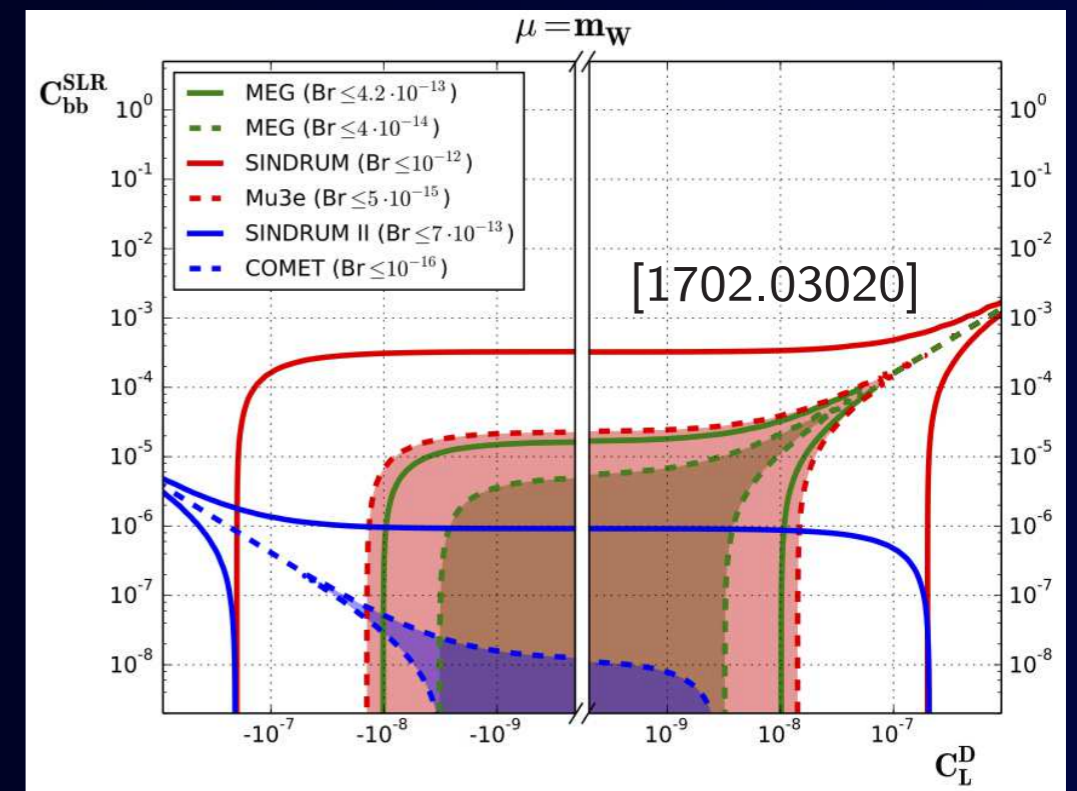
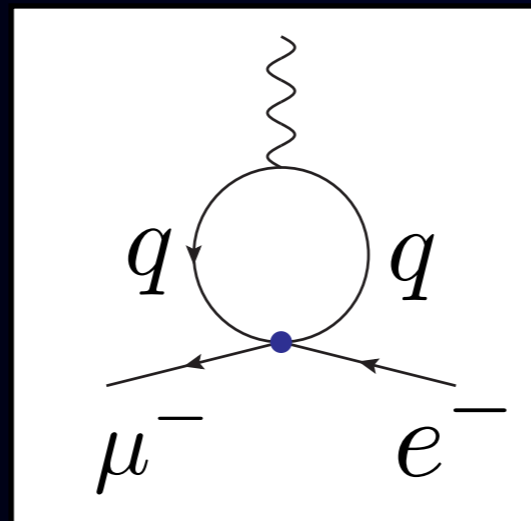
contact interaction



Operator Mixing via RGE

EFT at high physics scale

The operators are mixed in RGE at the experiment scale



2

All processes are equally important (not competing).

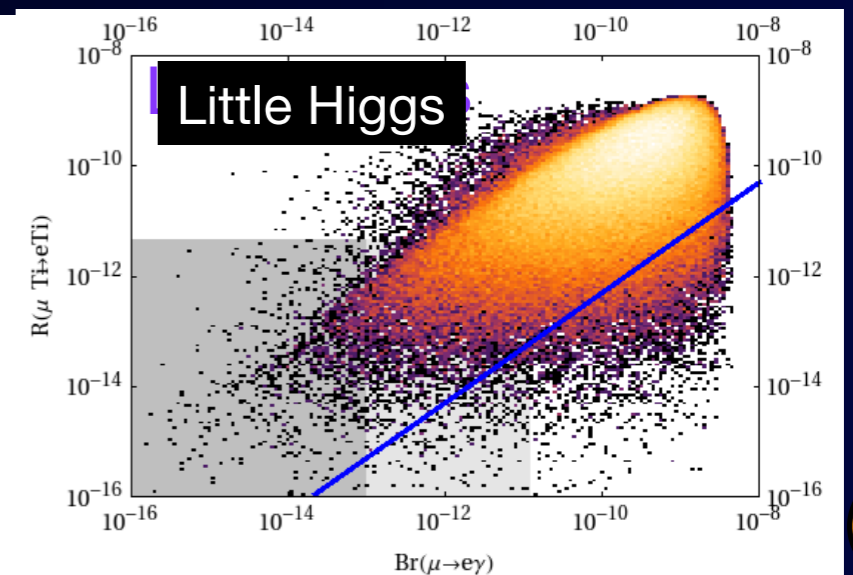
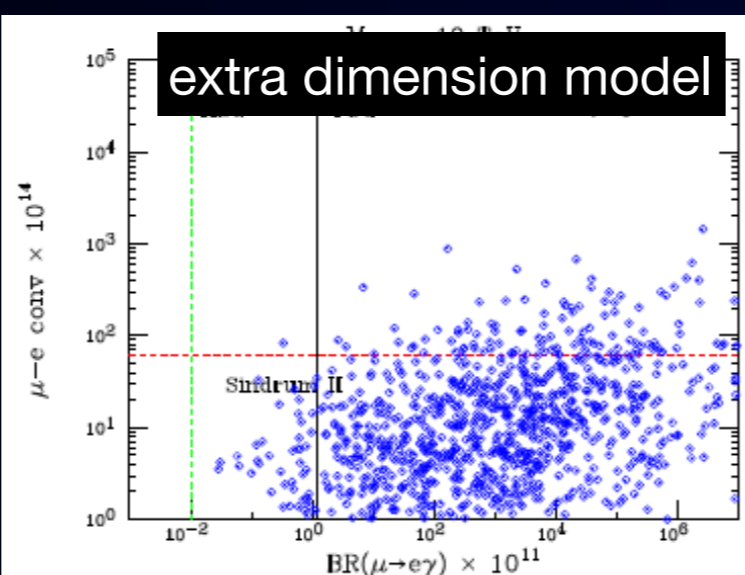
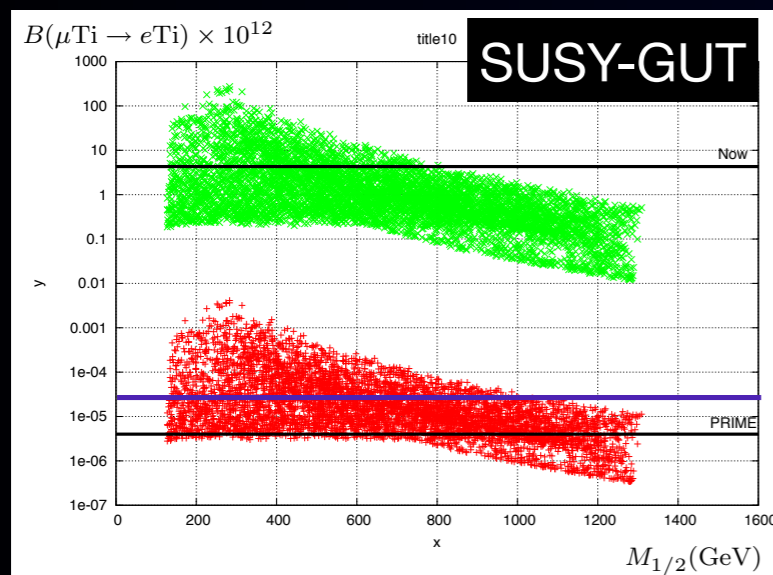
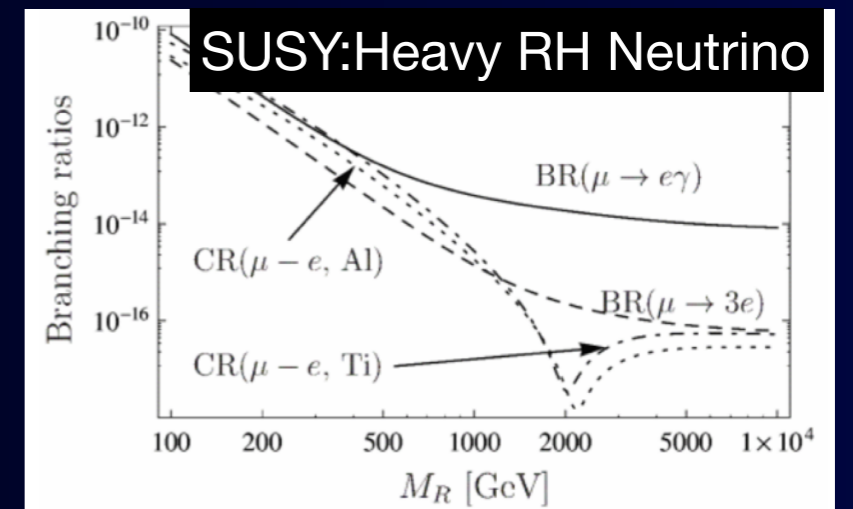
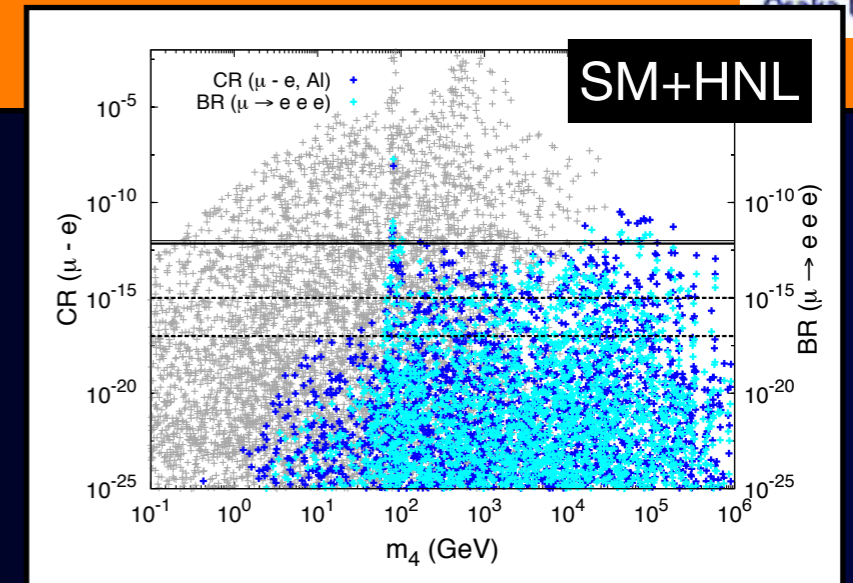
A. Crivellin, S. Davidson, G.M. Pruna and A. Signer, arXiv:1611.03409

A. Crivellin, S. Davidson, G.M. Pruna and A. Signer, JHEP 117 (2017) no.5

S. Davidson, Eur. Phys. J. C76 (2016) 370

Model dependent CLFV

- SM + NHL (neutral heavy lepton)
- large extra dimensions
- extended Higgs sector
- additional vector boson (Z')
- leptoquark
- SUSY-GUT and SUSY seesaw
- R-parity violating SUSY
- low-energy seesaw
- etc. etc.



Muon $g-2$ Anomaly and Muon CLFV

muon $g-2$ anomaly

flavour conserving component of the BSM dipole operator

muon CLFV ($\mu \rightarrow e\gamma$ etc.)

flavour violating component of the BSM dipole operator

If the Muon $g-2$ anomaly is confirmed, it will establish the presence of a BSM muon interaction which may induce sizable effects of muon CLFV.

Lepton Mixing
in the SM



Lepton Mixing in the Standard Model

*Neutral lepton flavour violation has been observed.
Lepton mixing in the SM has been known.*

Charged-current Interaction in the SM

$$\mathcal{L}_{\text{CC}} = -\frac{g}{\sqrt{2}} (\bar{e}_{aL} \gamma^\mu U_{ai} \nu_{iL}) W_\mu^- + h.c., \quad (a = e, \mu, \tau, \quad i = 1, 2, 3)$$

PMNS matrix $W^\dagger V = U$

$$|e_\beta\rangle = \sum_a W_{\beta a}^* |e_a\rangle, \quad |\nu_\beta\rangle = \sum_i V_{\beta i}^* |\nu_i\rangle, \quad e_a = e, \mu, \tau, \quad i = 1, 2, 3,$$

↑

flavour
eigenstate

↑

mass
eigenstate

↑

flavour
eigenstate

↑

mass
eigenstate

- The mass eigenstates and flavour eigenstates in the weak interaction are misaligned, as in the quark sector.

Neutrino Mixing



PMNS matrix $W^\dagger V = U$ $W = 1, V = U$

(charged lepton:
mass eigenstate)

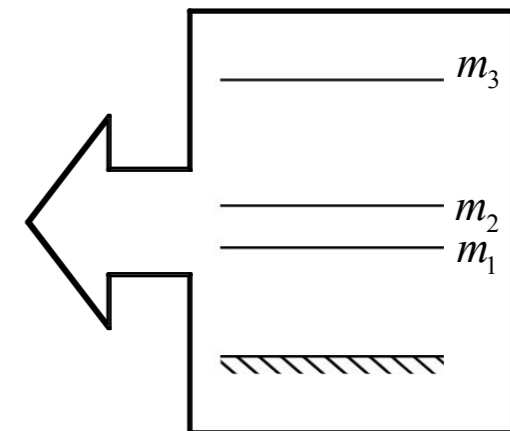
$$\begin{pmatrix} \nu_e \\ e^- \end{pmatrix}_L \quad \begin{pmatrix} \nu_\mu \\ \mu^- \end{pmatrix}_L \quad \begin{pmatrix} \nu_\tau \\ \tau^- \end{pmatrix}_L$$

Standard Model
states

neutrino
mixing matrix

$$\begin{pmatrix} \nu_e \\ \nu_\mu \\ \nu_\tau \end{pmatrix} = \begin{pmatrix} U_{e1} & U_{e2} & U_{e3} \\ U_{\mu1} & U_{\mu2} & U_{\mu3} \\ U_{\tau1} & U_{\tau2} & U_{\tau3} \end{pmatrix} \begin{pmatrix} \nu_1 \\ \nu_2 \\ \nu_3 \end{pmatrix}$$

Neutrino mass
states



$$U = \begin{pmatrix} 1 & 0 & 0 \\ 0 & c_{23} & s_{23} \\ 0 & -s_{23} & c_{23} \end{pmatrix} \begin{pmatrix} c_{13} & 0 & s_{13}e^{-i\delta} \\ 0 & 1 & 0 \\ -s_{13}e^{i\delta} & 0 & c_{13} \end{pmatrix} \begin{pmatrix} c_{12} & s_{12} & 0 \\ -s_{12} & c_{12} & 0 \\ 0 & 0 & 1 \end{pmatrix} \begin{pmatrix} e^{i\alpha_1/2} & 0 & 0 \\ 0 & e^{i\alpha_2/2} & 0 \\ 0 & 0 & 1 \end{pmatrix}$$

Atmospheric
angle

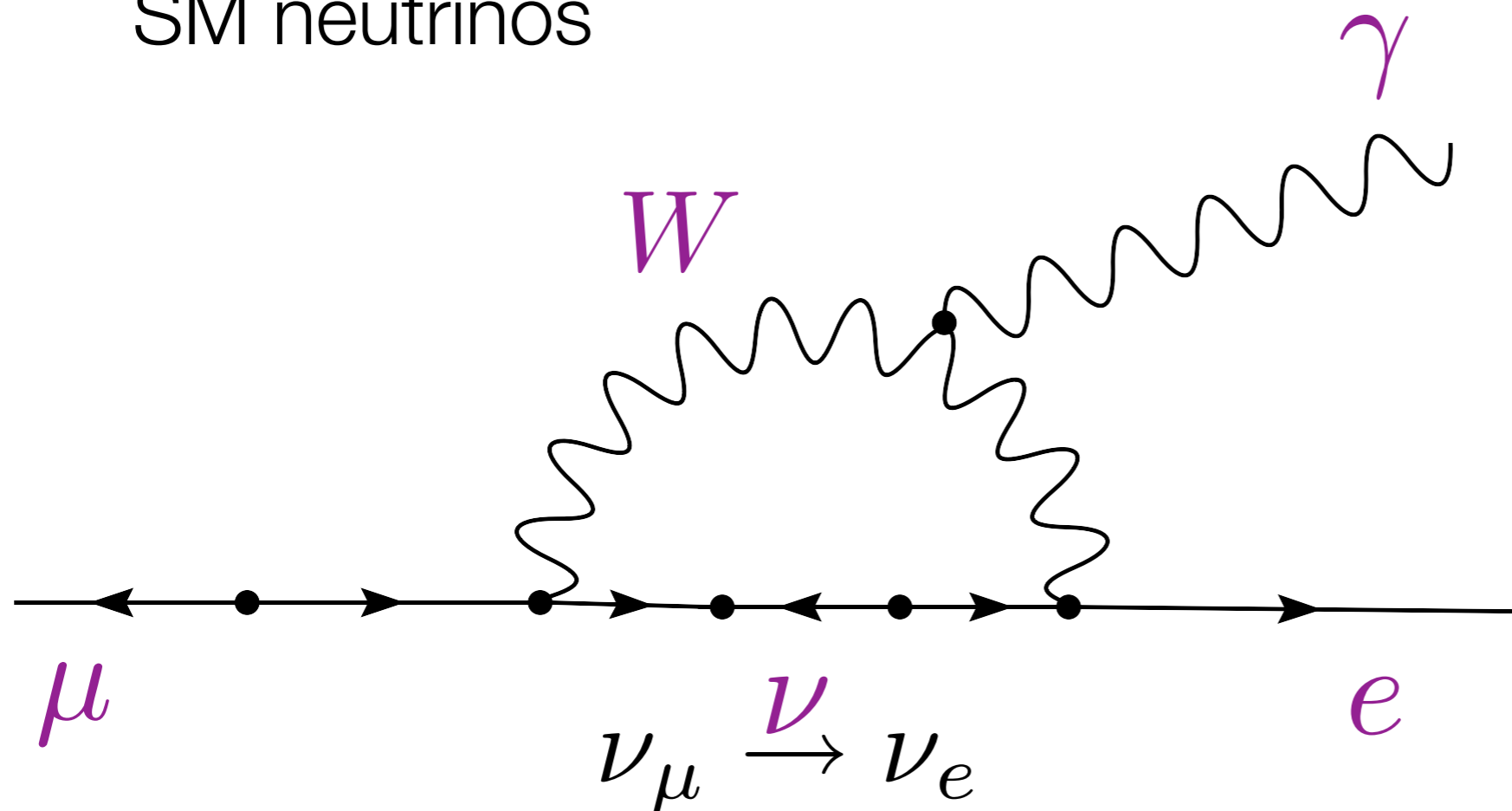
Reactor angle
and CP phase

Solar angle

Majorana phases

SM Contribution of Lepton Mixing to CLFV

SM neutrinos

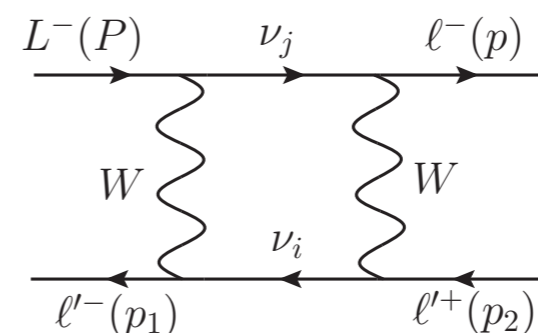
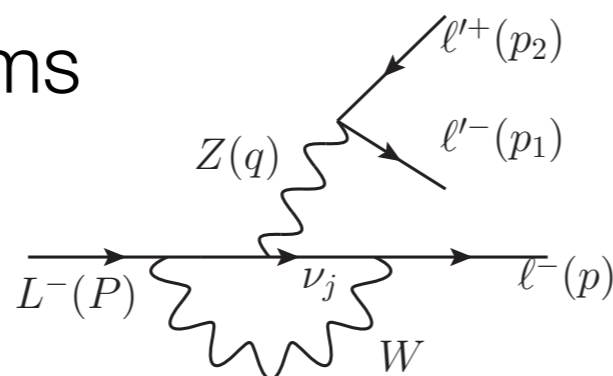


BR $\sim O(10^{-54})$

$$B(\mu \rightarrow e \gamma) = \frac{3\alpha}{32\pi} \left| \sum_l (V_{MNS})_{\mu l}^* (V_{MNS})_{el} \frac{m_{\nu_l}^2}{M_W^2} \right|^2$$

SM Contributions to $L^- \rightarrow \ell^- \ell'^+ \ell'^-$

Penguin diagrams



Box diagrams

Decay channel	Our Result	Petcov's Result*	Our Result	Petcov's Result*
$\mu^- \rightarrow e^- e^+ e^-$	$9,5 \cdot 10^{-55}$	$1,0 \cdot 10^{-53}$	$2,1 \cdot 10^{-56}$	$2,6 \cdot 10^{-53}$
$\tau^- \rightarrow e^- e^+ e^-$	$5,0 \cdot 10^{-56}$	$1,8 \cdot 10^{-54}$	$3,6 \cdot 10^{-57}$	$4,5 \cdot 10^{-54}$
$\tau^- \rightarrow \mu^- \mu^+ \mu^-$	$1,0 \cdot 10^{-54}$	$3,7 \cdot 10^{-53}$	$7,6 \cdot 10^{-56}$	$9,7 \cdot 10^{-53}$
$\tau^- \rightarrow e^- \mu^+ \mu^-$	$2,9 \cdot 10^{-56}$	$1,0 \cdot 10^{-54}$	$1,7 \cdot 10^{-57}$	$2,2 \cdot 10^{-54}$
$\tau^- \rightarrow \mu^- e^+ e^-$	$7,3 \cdot 10^{-55}$	$2,5 \cdot 10^{-53}$	$4,0 \cdot 10^{-56}$	$5,0 \cdot 10^{-53}$

Total

Decay channel	Our Result	Petcov's Result*
$\mu^- \rightarrow e^- e^+ e^-$	$7,4 \cdot 10^{-55}$	$8,5 \cdot 10^{-54}$
$\tau^- \rightarrow e^- e^+ e^-$	$3,2 \cdot 10^{-56}$	$1,4 \cdot 10^{-54}$
$\tau^- \rightarrow \mu^- \mu^+ \mu^-$	$6,4 \cdot 10^{-55}$	$3,2 \cdot 10^{-53}$
$\tau^- \rightarrow e^- \mu^+ \mu^-$	$2,1 \cdot 10^{-56}$	$9,4 \cdot 10^{-55}$
$\tau^- \rightarrow \mu^- e^+ e^-$	$5,2 \cdot 10^{-55}$	$2,1 \cdot 10^{-53}$

S. T. Petcov, Sov. J. Nucl. Phys. 25, 340 (1977).

G. Hernandez-Tome, G. Lopez-Castro and P. Roig. ArXiv:1807.0605

Neutrino Oscillation

- Consider a particular neutrino flavour eigenstate, $|\nu_\alpha\rangle = \sum_i U_{\beta i}^* |\nu_i\rangle$, created at some point in time by weak interactions,
- During the propagation, the different mass eigenstates accumulate “phase”, depending on their mass. $|\nu_\alpha\rangle = \sum_i \exp(-ip_i x) U_{\beta i}^* |\nu_i\rangle$
- At the detector, a particular flavour eigenstate is measured (disappearance, or appearance).

$$P(\nu_l \rightarrow \nu_m) = \left| \sum_j V_{mj} V_{lj}^* \exp\left(-i \frac{m_j^2 L}{2E}\right) \right|^2$$

2 flavor approximation:

$$P(\nu_l \rightarrow \nu_m) = \sin^2(2\theta) \sin^2\left(\frac{\Delta m^2 L}{4E}\right) \quad \Delta m_{32}^2 \sim 10^{-3} \text{eV}^2$$

$$P(\nu_l \rightarrow \nu_l) = 1 - \sin^2(2\theta) \sin^2\left(\frac{\Delta m^2 L}{4E}\right)$$

Charged Lepton Oscillation

PMNS matrix $W^\dagger V = U$ $W = U, V = 1$

(charged lepton:
flavour eigenstate)

$$|e_1\rangle = U_{1e}|e\rangle + U_{1\mu}|\mu\rangle + U_{1\tau}|\tau\rangle,$$

$$|e_2\rangle = U_{2e}|e\rangle + U_{2\mu}|\mu\rangle + U_{2\tau}|\tau\rangle,$$

$$|e_3\rangle = U_{3e}|e\rangle + U_{3\mu}|\mu\rangle + U_{3\tau}|\tau\rangle,$$



flavour eigenstate



mass eigenstate

- When neutrinos produced in weak interactions are mass eigenstates, the associated charged leptons are flavour eigenstates as shown above (like EPR)
- Then, **do charged leptons oscillate among them ?**

Homework 1



- Consider a question of a hypothetical experiment (“gedanken”), what is the requirements to make “charged lepton oscillation” happening ?
- Consider how can the superposition of mass eigenstates of charged leptons (flavour eigenstates) be created ?

S. Pakvasa, Letter at Nuovo Cimento, Vol.31, 15 (1981) 8

Evgeny. Kh Akhmedov, JHEP 09 (2009) 116

Homework 2



- Consider again a question of thought experiments (“gedanken”). If we can measure the neutrino mass eigenstate (not flavour eigenstate) at the detector, how would the neutrino oscillation measured be modified ?

More CLFV



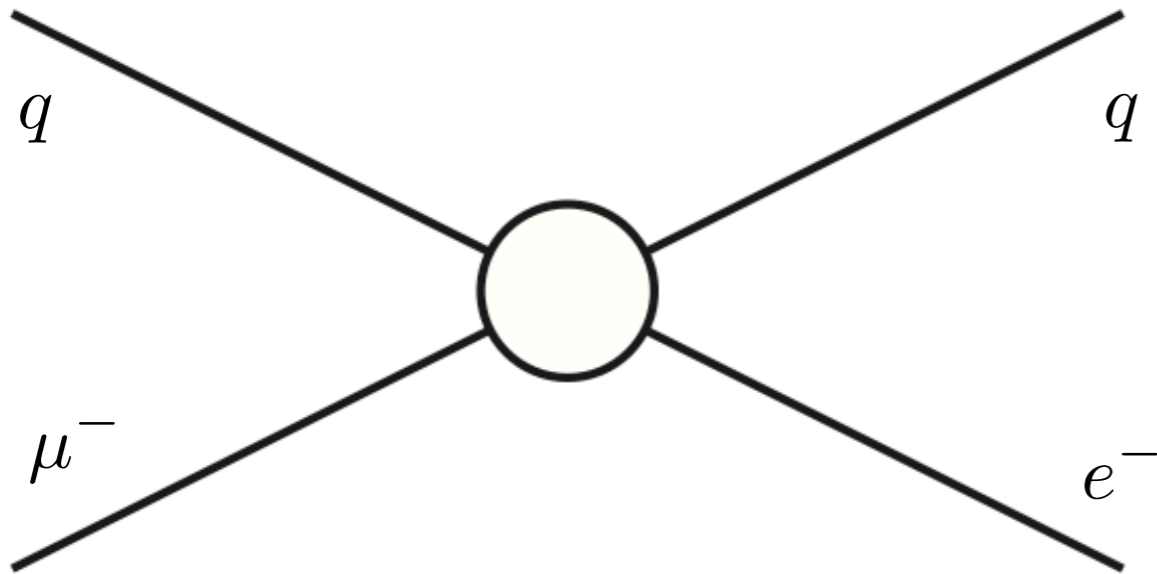
CLFV Processes

- $\mu^+ \rightarrow e^+ \gamma$
- $\mu^+ \rightarrow e^+ e^+ e^-$
- $\mu^- + N(A, Z) \rightarrow e^- + N(A, Z)$
- $\mu^- + N(A, Z) \rightarrow e^+ + N(A, Z - 2)$
- $\mu^- + N(A, Z) \rightarrow \mu^+ + N(A, Z - 2)$
- $\mu^+ e^- \rightarrow \mu^- e^+$
- $\mu^- e^- \rightarrow e^- e^-$
- $\mu + N \rightarrow \tau + X$
- $\nu_\mu + N \rightarrow \tau^\pm + X$

EFT approach for $\mu \rightarrow e$ conversion

$$\mu^- + q \rightarrow e^- + q$$

contact interaction

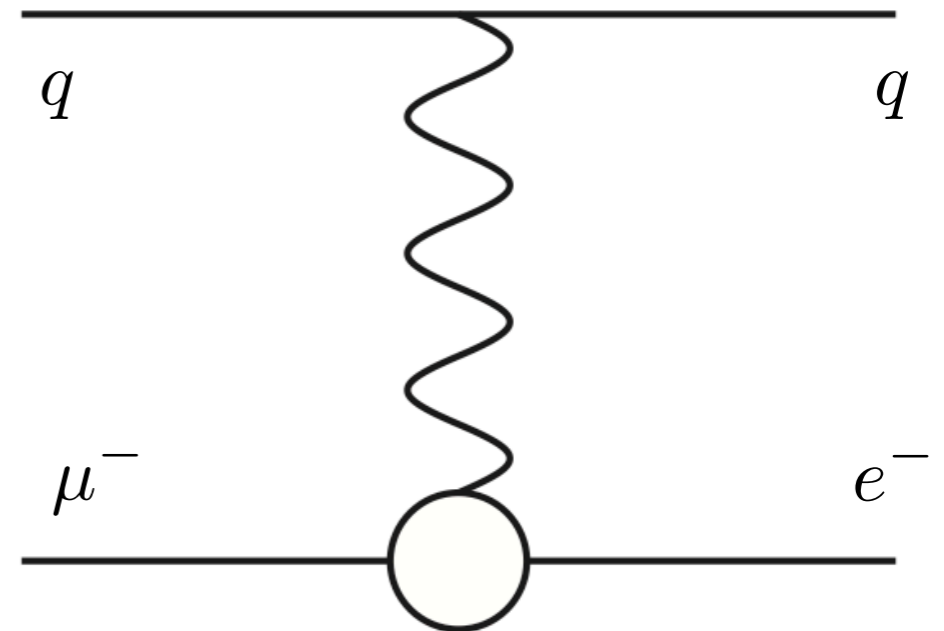


$$(\bar{e}\Gamma P_Y \mu)(\bar{q}\Gamma q) \quad , \quad q \in \{u, d, s\}$$

$$\Gamma = \{I, \gamma_5, \gamma, \gamma\gamma_5, \sigma\}$$

S, P, V, A, T

dipole interaction



dipole (D)

Effective Field Theory for $\mu \rightarrow e$ Conversion

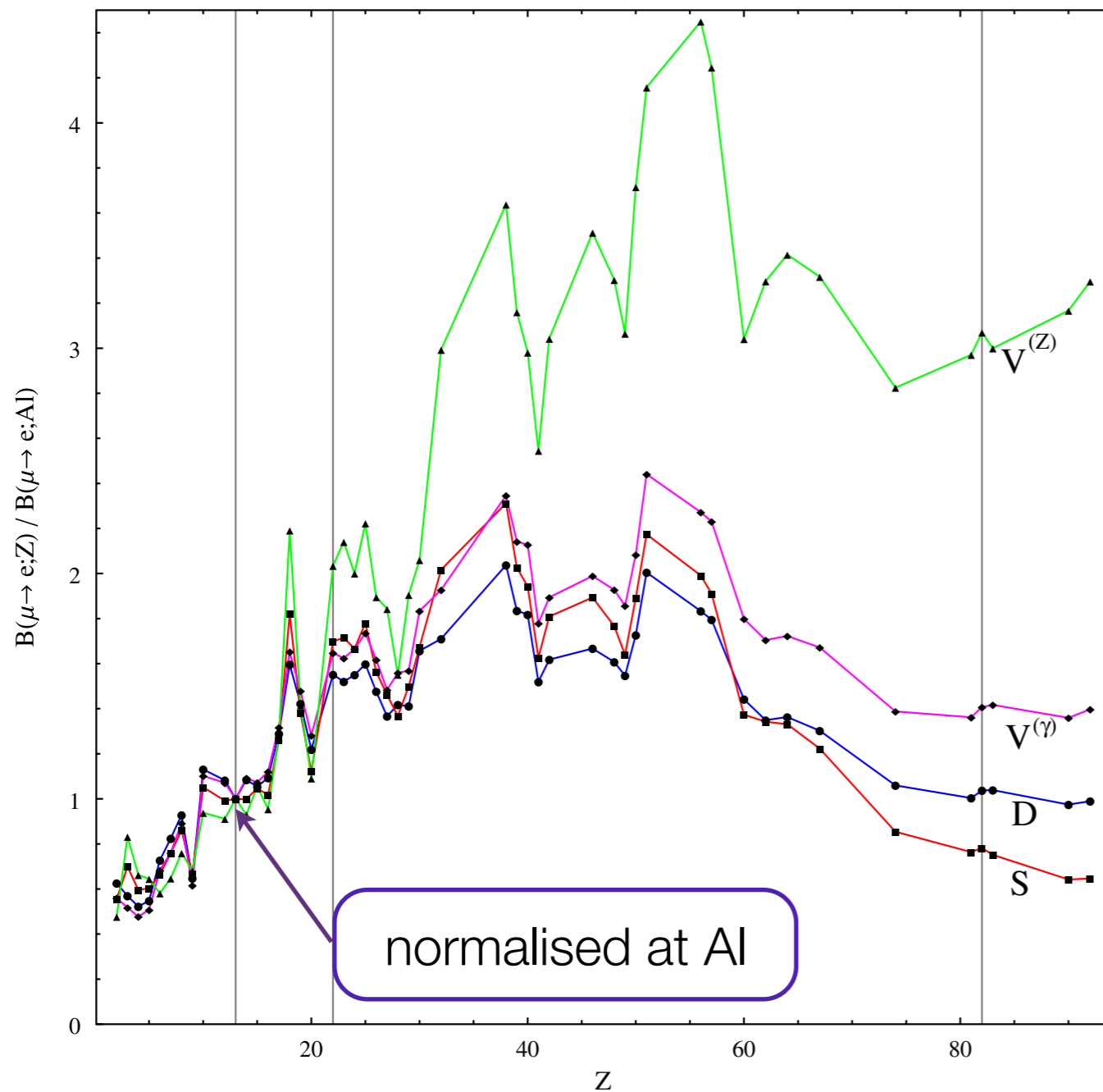


two-lepton and two-nucleon operators and dipole operators

$$\begin{aligned}
 \mathcal{L}_{\mu A \rightarrow e A}(\Lambda_{expt}) = & -\frac{4G_F}{\sqrt{2}} \sum_{N=p,n} \left[m_\mu (C_{DL} \bar{e}_R \sigma^{\alpha\beta} \mu_L F_{\alpha\beta} + C_{DR} \bar{e}_L \sigma^{\alpha\beta} \mu_R F_{\alpha\beta}) \right. \\
 \text{scalar} & + \left(\tilde{C}_{SL}^{(NN)} \bar{e} P_L \mu + \tilde{C}_{SR}^{(NN)} \bar{e} P_R \mu \right) \bar{N} N \\
 \text{pseudo-scalar} & + \left(\tilde{C}_{P,L}^{(NN)} \bar{e} P_L \mu + \tilde{C}_{P,R}^{(NN)} \bar{e} P_R \mu \right) \bar{N} \gamma_5 N \\
 \text{vector} & + \left(\tilde{C}_{VL}^{(NN)} \bar{e} \gamma^\alpha P_L \mu + \tilde{C}_{VR}^{(NN)} \bar{e} \gamma^\alpha P_R \mu \right) \bar{N} \gamma_\alpha N \\
 \text{axial-vector} & + \left(\tilde{C}_{A,L}^{(NN)} \bar{e} \gamma^\alpha P_L \mu + \tilde{C}_{A,R}^{(NN)} \bar{e} \gamma^\alpha P_R \mu \right) \bar{N} \gamma_\alpha \gamma_5 N \\
 \text{(derivative)} & + \left(\tilde{C}_{Der,L}^{(NN)} \bar{e} \gamma^\alpha P_L \mu + \tilde{C}_{Der,R}^{(NN)} \bar{e} \gamma^\alpha P_R \mu \right) i (\bar{N} \overleftrightarrow{\partial}_\alpha \gamma_5 N) \\
 \text{tensor} & + \left(\tilde{C}_{T,L}^{(NN)} \bar{e} \sigma^{\alpha\beta} P_L \mu + \tilde{C}_{T,R}^{(NN)} \bar{e} \sigma^{\alpha\beta} P_R \mu \right) \bar{N} \sigma_{\alpha\beta} N + h.c. \left. \right] .
 \end{aligned}$$

dipole

Discrimination of the interactions by different targets



vector interaction
(with Z boson)

with Z penguin

vector interaction
(with photon -
charge radius)

left-right models

dipole interaction

SUSY-GUT

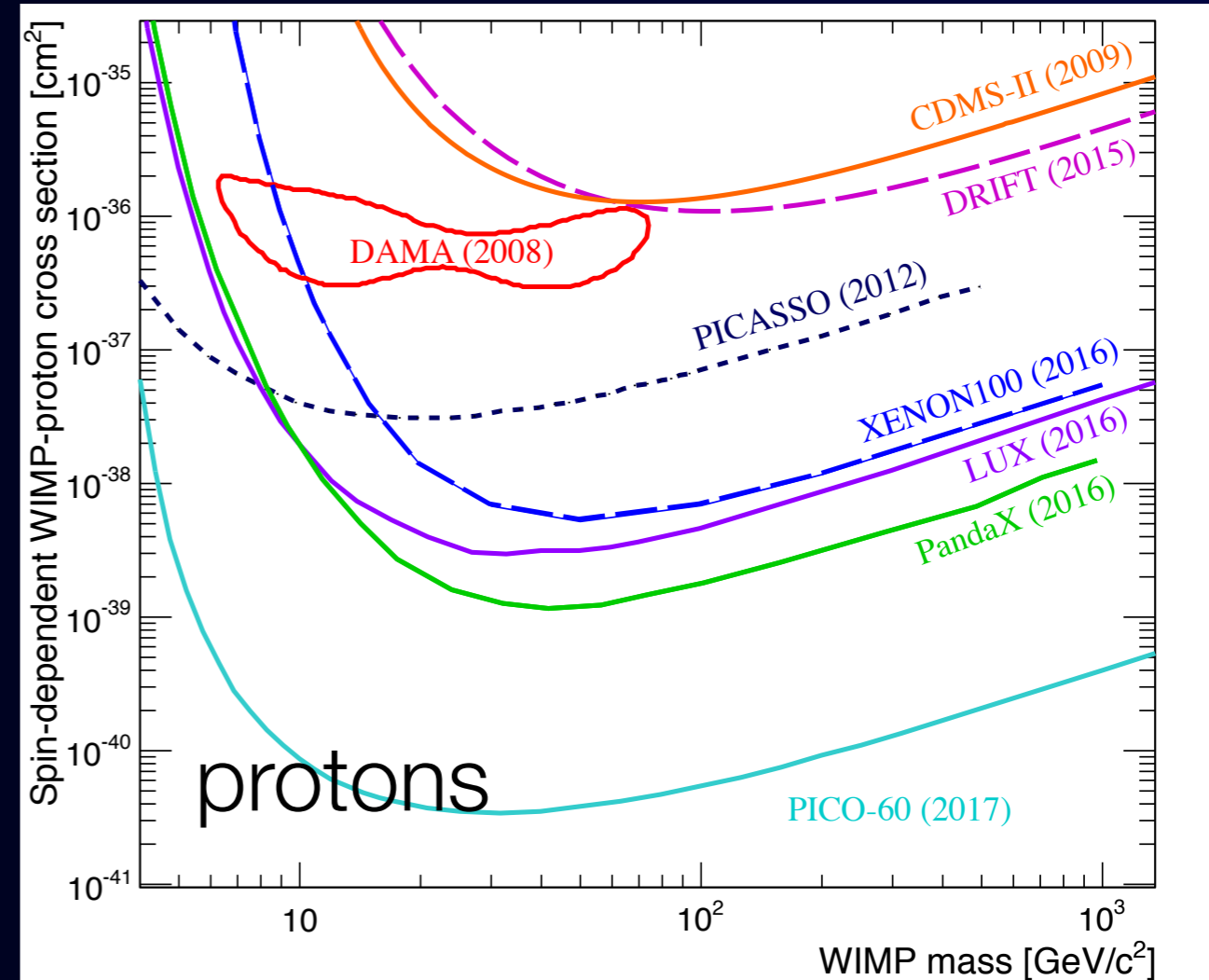
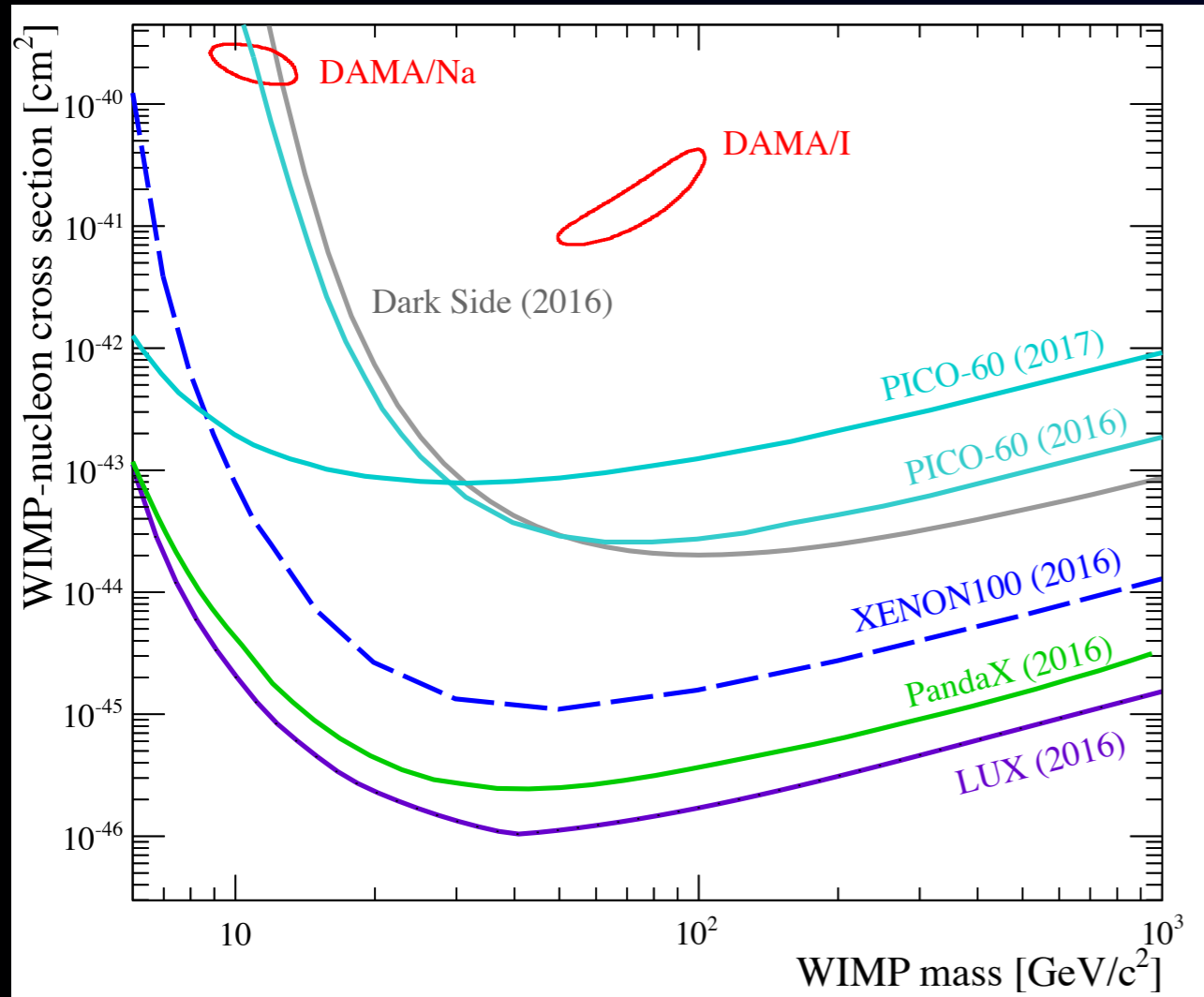
scalar interaction

SUSY seesaw

R. Kitano, M. Koike and Y. Okada, Phys.Rev. D66 (2002) 096002; D76 (2007) 059902
 V. Cirigliano, R. Kitano, Y. Okada, and P. Tuzon, Phys. Rev. D80 (2009) 013002

WIMP Searches

Spin-Independent and Spin-dependent



spin-independent cross section
scalar, vector interaction

spin-dependent cross section
pseudo-scalar, axial-vector,
tensor interactions

Spin Dependent μ -e conversion and Spin Independent μ -e conversion



dipole
interaction

vector
interaction

scalar
interaction

Spin independent
 μ -e Conversion
(coherent)

Pseudo-
scaler
interaction

axial vector
interaction

tensor
interaction

Spin dependent
 μ -e Conversion
(incoherent)

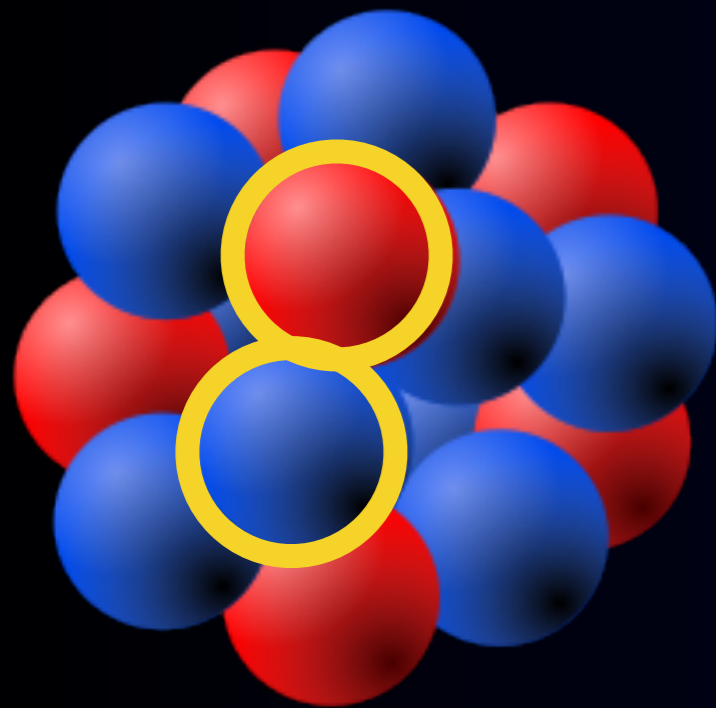
compare zero-spin and non-zero-spin nuclear targets

V. Cirigliano, S. Davidson, YK, Phys. Lett. B 771 (2017) 242

S. Davidson, YK, A. Saporta, Eur. Phys. J. C78 (2018) 109

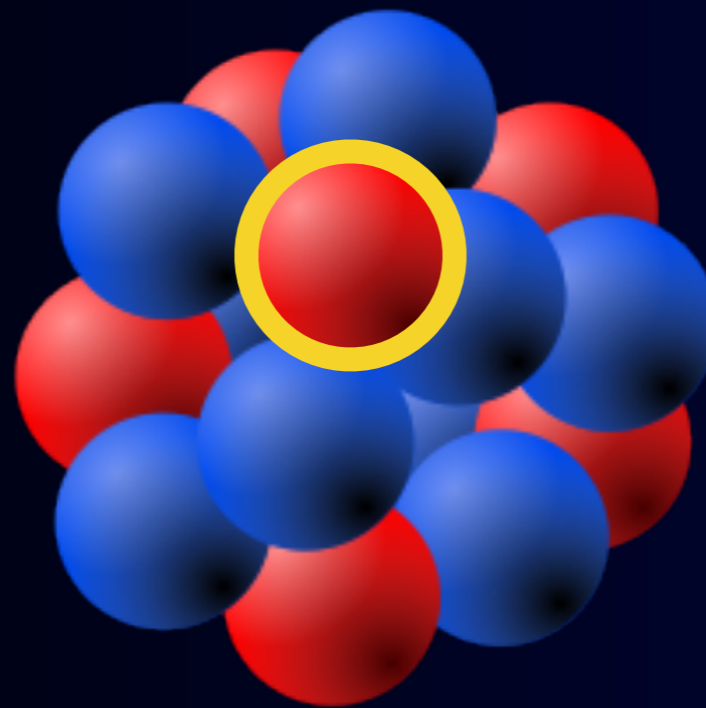
Coherent and Incoherent : Pros and Cons

Coherent
 μ -e Conversion
(spin independent)



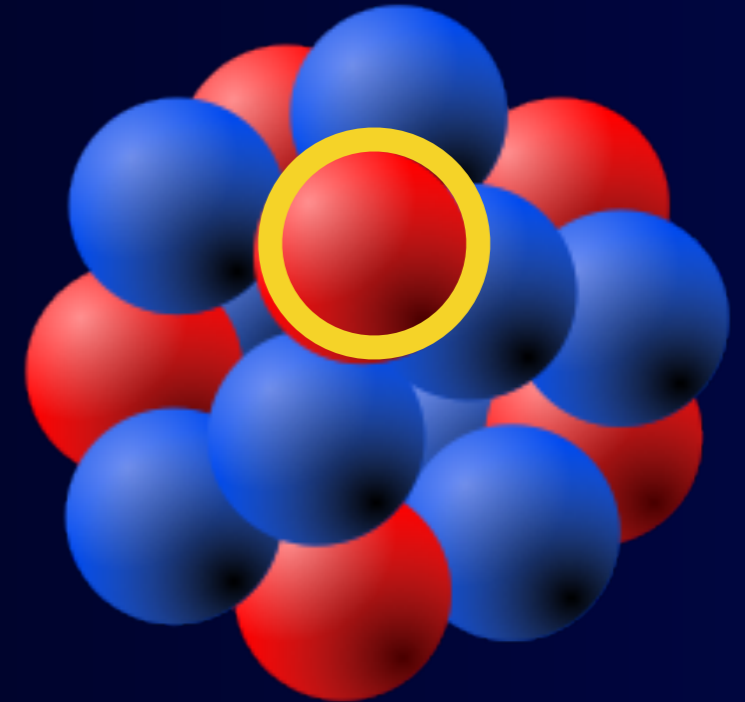
$$|\sum_i N_i|^2 \propto A^2$$

nuclear muon
capture



$$\sum_i |N_i|^2 \propto Z$$

Incoherent
 μ -e Conversion
(spin dependent)



$$|N_i|^2 \propto 1$$



Contents lists available at [ScienceDirect](#)

Physics Letters B

www.elsevier.com/locate/physletb



Spin-dependent $\mu \rightarrow e$ conversion



Vincenzo Cirigliano^a, Sacha Davidson^{b,*}, Yoshitaka Kuno^c

^a *Theoretical Division, Los Alamos National Laboratory, Los Alamos, NM 87545, USA*

^b *IPNL, CNRS/IN2P3, Université Lyon 1, Univ. Lyon, 69622 Villeurbanne, France*

^c *Department of Physics, Osaka University, 1-1 Machikaneyama, Toyonaka, Osaka 560-0043, Japan*

ARTICLE INFO

Article history:

Received 16 March 2017

Received in revised form 6 May 2017

Accepted 19 May 2017

Available online 22 May 2017

Editor: J. Hisano

ABSTRACT

The experimental sensitivity to $\mu \rightarrow e$ conversion on nuclei is expected to improve by four orders of magnitude in coming years. We consider the impact of $\mu \rightarrow e$ flavour-changing tensor and axial-vector four-fermion operators which couple to the spin of nucleons. Such operators, which have not previously been considered, contribute to $\mu \rightarrow e$ conversion in three ways: in nuclei with spin they mediate a spin-dependent transition; in all nuclei they contribute to the coherent (A^2 -enhanced) spin-independent conversion via finite recoil effects and via loop mixing with dipole, scalar, and vector operators. We estimate the spin-dependent rate in Aluminium (the target of the upcoming COMET and Mu2e experiments), show that the loop effects give the greatest sensitivity to tensor and axial-vector operators involving first-generation quarks, and discuss the complementarity of the spin-dependent and independent contributions to $\mu \rightarrow e$ conversion.

© 2017 The Author(s). Published by Elsevier B.V. This is an open access article under the CC BY license

“Spin-dependent” $\mu \rightarrow e$ conversion on light nuclei

Sacha Davidson^{1,2,3,a}, Yoshitaka Kuno⁴, Albert Saporta^{1,2,3}

¹ IPNL, CNRS/IN2P3, 4 Rue E. Fermi, 69622 Villeurbanne Cedex, France

² Université Claude Bernard Lyon 1, Villeurbanne, France

³ Université de Lyon, 69622 Lyon, France

⁴ Department of Physics, Osaka University, 1-1 Machikaneyama, Toyonaka, Osaka 560-0043, Japan

Received: 25 October 2017 / Accepted: 23 January 2018 / Published online: 6 February 2018

© The Author(s) 2018. This article is an open access publication

Abstract The experimental sensitivity to $\mu \rightarrow e$ conversion will improve by four or more orders of magnitude in coming years, making it interesting to consider the “spin-dependent” (SD) contribution to the rate. This process does not benefit from the atomic-number-squared enhancement of the spin-independent (SI) contribution, but probes different operators. We give details of our recent estimate of the spin-dependent rate, expressed as a function of opera-

the μ is captured by a nucleus, and can convert to an electron while in orbit. The COMET [7] and Mu2e [8] experiments, currently under construction, plan to improve the sensitivity by four orders of magnitude, reaching a branching ratio $\sim 10^{-16}$. The PRISM/PRIME proposal [9] aims to probe $\sim 10^{-18}$. These exceptional improvements in experimental sensitivity motivate our interest in subdominant contributions to $\mu \rightarrow e$ conversion.

EFT for $\mu \rightarrow e$ Conversion

$$\begin{aligned}
 \mathcal{L}_{\mu A \rightarrow e A}(\Lambda_{expt}) = & -\frac{4G_F}{\sqrt{2}} \sum_{N=p,n} \left[m_\mu (C_{DL} \bar{e}_R \sigma^{\alpha\beta} \mu_L F_{\alpha\beta} + C_{DR} \bar{e}_L \sigma^{\alpha\beta} \mu_R F_{\alpha\beta}) \right. \\
 & \text{dipole} \\
 \text{scalar} & + \left(\tilde{C}_{SL}^{(NN)} \bar{e} P_L \mu + \tilde{C}_{SR}^{(NN)} \bar{e} P_R \mu \right) \bar{N} N \\
 \text{pseudo-scalar} & + \left(\tilde{C}_{P,L}^{(NN)} \bar{e} P_L \mu + \tilde{C}_{P,R}^{(NN)} \bar{e} P_R \mu \right) \bar{N} \gamma_5 N \\
 \text{vector} & + \left(\tilde{C}_{VL}^{(NN)} \bar{e} \gamma^\alpha P_L \mu + \tilde{C}_{VR}^{(NN)} \bar{e} \gamma^\alpha P_R \mu \right) \bar{N} \gamma_\alpha N \\
 \text{axial-vector} & + \left(\tilde{C}_{A,L}^{(NN)} \bar{e} \gamma^\alpha P_L \mu + \tilde{C}_{A,R}^{(NN)} \bar{e} \gamma^\alpha P_R \mu \right) \bar{N} \gamma_\alpha \gamma_5 N \\
 \text{(derivative)} & + \left(\tilde{C}_{Der,L}^{(NN)} \bar{e} \gamma^\alpha P_L \mu + \tilde{C}_{Der,R}^{(NN)} \bar{e} \gamma^\alpha P_R \mu \right) i (\bar{N} \overleftrightarrow{\partial}_\alpha \gamma_5 N) \\
 \text{tensor} & + \left. \left(\tilde{C}_{T,L}^{(NN)} \bar{e} \sigma^{\alpha\beta} P_L \mu + \tilde{C}_{T,R}^{(NN)} \bar{e} \sigma^{\alpha\beta} P_R \mu \right) \bar{N} \sigma_{\alpha\beta} N + h.c. \right] .
 \end{aligned}$$

let us make an argument simplified...

5 coeff. - dipole, scalar (p), vector (p), scalar (n), vector (n)

Past Measurements



Table 1

Current experimental bounds on $\mu \rightarrow e$ conversion (the last line gives the future sensitivity on Aluminium), and parameters relevant to the SD calculation. The isotope abundances are from [29]. The parameter B_Z is defined in eqn. (8). The estimate for S_p^{Au} is based on the Odd Group Model of [24], assuming $J = 1/2$. The estimated form factors $S_I(m_\mu)/S_I(0)$ for Titanium and Lead are an extrapolation from [11], discussed in the Appendix.

Target	Isotopes [abundance]	J	S_p^A, S_n^A	$S_I(m_\mu)/S_I(0)$	B_Z	BR (90% C.L.)
Sulfur	$Z = 16, A = 32$ [95%]	0				$< 7 \times 10^{-11}$ [23]
Titanium	$Z = 22, A = 48$ [74%]	0			234	$< 4.3 \times 10^{-12}$ [17]
	$Z = 22, A = 47$ [7.5%]	5/2	0.0, 0.21 [24]	~ 0.12		
	$Z = 22, A = 49$ [5.4%]	7/2	0.0, 0.29 [24]	~ 0.12		
Copper	$Z = 29, A = 63$ [70%]	3/2				$BR \leq 1.6 \times 10^{-8}$ [25]
	$Z = 29, A = 65$ [31%]	3/2				
Gold	$Z = 79, A = 197$ [100%]	5/2	$-(0.52 \rightarrow 0.30), 0.0$		285	$BR < 7 \times 10^{-13}$ [17]
Lead	$Z = 82, A = 206$ [24%]	0				$BR < 4.6 \times 10^{-11}$ [17]
	$Z = 82, A = 207$ [22%]	1/2	0.0, -0.15 [24]	0.55 [28], $\sim .026$		
	$Z = 82, A = 208$ [52%]	0				
Aluminium	$Z = 13, A = 27$ [100%]	5/2	0.34, 0.030 [21,22]	0.29 [21,22]	132	$\rightarrow 10^{-16}$

Conversion Rate Calculations

$$\text{BR}_{SI}(\mu A \rightarrow eA) = \frac{32G_F^2 m_\mu^5}{\Gamma_{cap}} \left[\left| \tilde{C}_{V,R}^{pp} V^{(p)} + \tilde{C}_{S,L}^{pp'} S^{(p)} + \tilde{C}_{V,R}^{nn} V^{(n)} + \tilde{C}_{S,L}^{nn'} S^{(n)} + C_{D,L} \frac{D}{4} \right|^2 + \{L \leftrightarrow R\} \right], \quad (2)$$

$$\begin{aligned} \text{BR}_{SD}(\mu A \rightarrow eA) &= \frac{8G_F^2 m_\mu^5 (\alpha Z)^3}{\Gamma_{cap} \pi^2} \left[\sum_I 4\epsilon_I \frac{J_I + 1}{J_I} \left| S_p^I (\tilde{C}_{A,L}^{pp} + 2\tilde{C}_{T,R}^{pp}) + S_n^I (\tilde{C}_{A,L}^{nn} + 2\tilde{C}_{T,R}^{nn}) \right|^2 \frac{S_I(m_\mu)}{S_I(0)} + \{L \leftrightarrow R\} \right] \end{aligned}$$

Vector presentation in multi-dimension space (5-dim.)



KITANO, KOIKE, AND OKADA

PHYSICAL REVIEW D **66**, 096002 (2002)

TABLE I. The overlap integrals in units of $m_\mu^{5/2}$ are listed. The proton distributions in the nuclei are taken from Ref. [20] (see also Appendix A), and neutron distributions are assumed to be the same as those of the protons (method 1 in Sec. III A).

Nucleus	D	$S^{(p)}$	$V^{(p)}$	$S^{(n)}$	$V^{(n)}$
${}^4_2\text{He}$	0.000625	0.000262	0.000263	0.000262	0.000263
${}^7_3\text{Li}$	0.00138	0.000581	0.000585	0.000775	0.000780
${}^9_4\text{Be}$	0.00268	0.00113	0.00114	0.00141	0.00142
${}^{11}_5\text{B}$	0.00472	0.00200	0.00202	0.00240	0.00242
${}^{12}_6\text{C}$	0.00724	0.00308	0.00312	0.00308	0.00312
${}^{14}_7\text{N}$	0.0103	0.0044	0.0044	0.0044	0.0044
${}^{16}_8\text{O}$	0.0133	0.0057	0.0058	0.0057	0.0058
${}^{19}_9\text{F}$	0.0166	0.0071	0.0072	0.0079	0.0081
${}^{20}_{10}\text{Ne}$	0.0205	0.0088	0.0090	0.0088	0.0090
${}^{24}_{12}\text{Mg}$	0.0312	0.0133	0.0138	0.0133	0.0138
${}^{27}_{13}\text{Al}$	0.0362	0.0155	0.0161	0.0167	0.0173
${}^{28}_{14}\text{Si}$	0.0419	0.0179	0.0187	0.0179	0.0187
${}^{31}_{15}\text{P}$	0.0468	0.0201	0.0210	0.0214	0.0224
${}^{32}_{16}\text{S}$	0.0524	0.0225	0.0236	0.0225	0.0236
${}^{35}_{17}\text{Cl}$	0.0565	0.0241	0.0254	0.0256	0.0269
${}^{40}_{18}\text{Ar}$	0.0621	0.0265	0.0281	0.0324	0.0343
${}^{39}_{19}\text{K}$	0.0699	0.0299	0.0317	0.0314	0.0334
${}^{40}_{20}\text{Ca}$	0.0761	0.0325	0.0347	0.0325	0.0347
${}^{48}_{22}\text{Ti}$	0.0864	0.0368	0.0396	0.0435	0.0468
${}^{51}_{23}\text{V}$	0.0931	0.0396	0.0428	0.0482	0.0521
${}^{52}_{24}\text{Cr}$	0.100	0.0425	0.0461	0.0496	0.0538

Vector presentation in multi-dimension space (5-dim.)



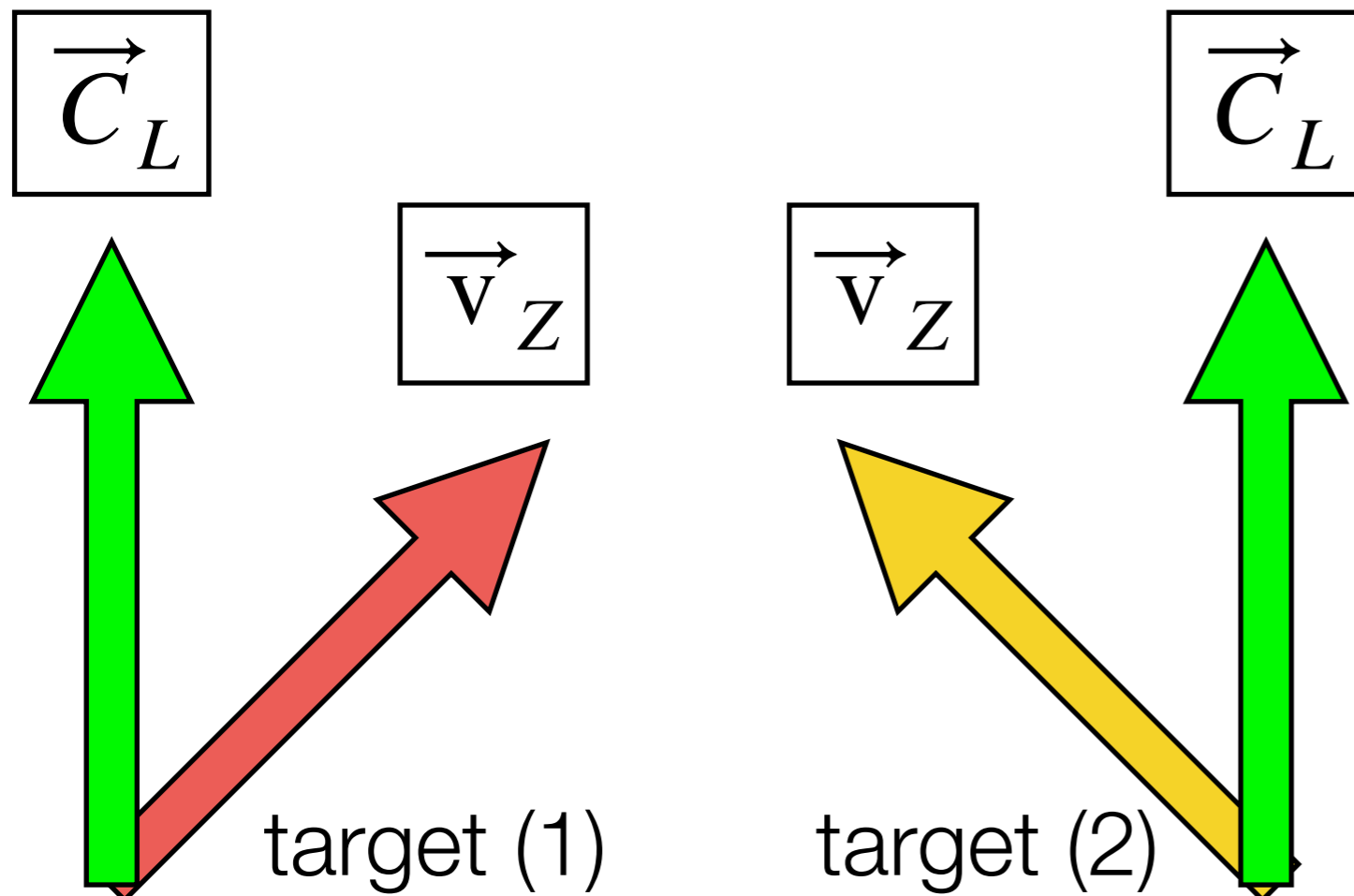
$$BR = B_Z \left[|\vec{v}_Z \cdot \vec{C}_L|^2 + |\vec{v}_Z \cdot \vec{C}_R|^2 \right]$$

$$\vec{C}_L = (\tilde{C}_{D,R}, \tilde{C}_{V,L}^{pp}, \tilde{C}_{S,R}^{pp}, \tilde{C}_{V,L}^{nn}, \tilde{C}_{S,R}^{nn}) \quad \text{new physics}$$

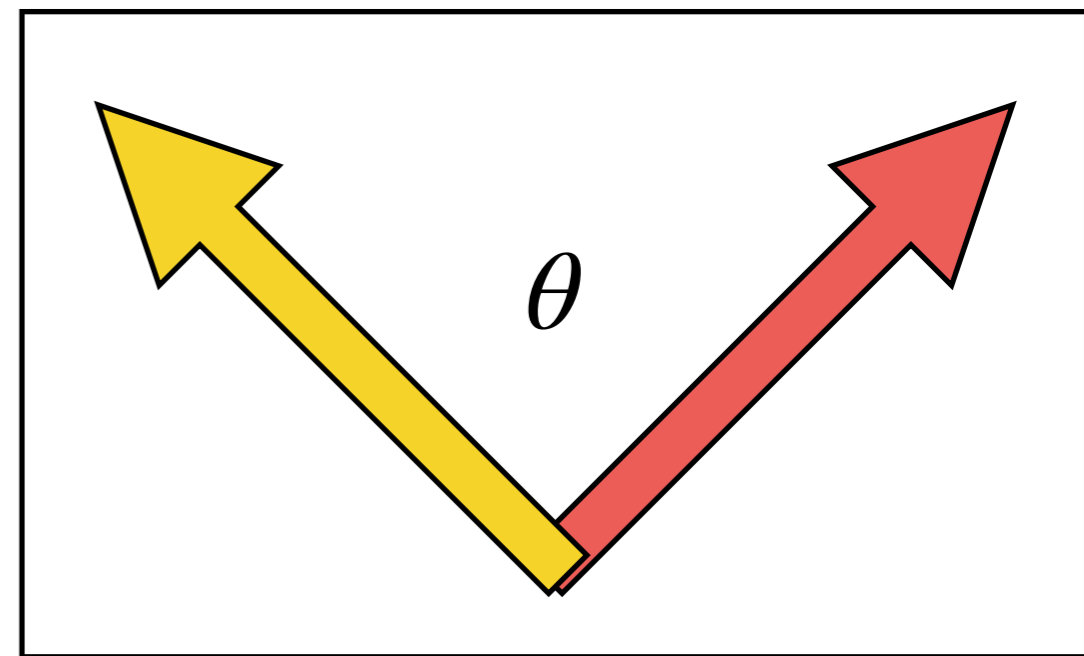
$$\vec{v}_Z = \left(\frac{D_Z}{4}, V_Z^{(p)}, S_Z^{(p)}, V_Z^{(n)}, S_Z^{(n)} \right) \quad \text{nuclear form factor}$$

Nuclear form factors, including
overlap of muon wave function and nucleus
calculated by nuclear physics
(estimated by WINP searches)

Misalignment is needed....



misalignment of target vectors provide more information on couplings



Spin dependent μ -e conversion (Model Independent) - second preprint

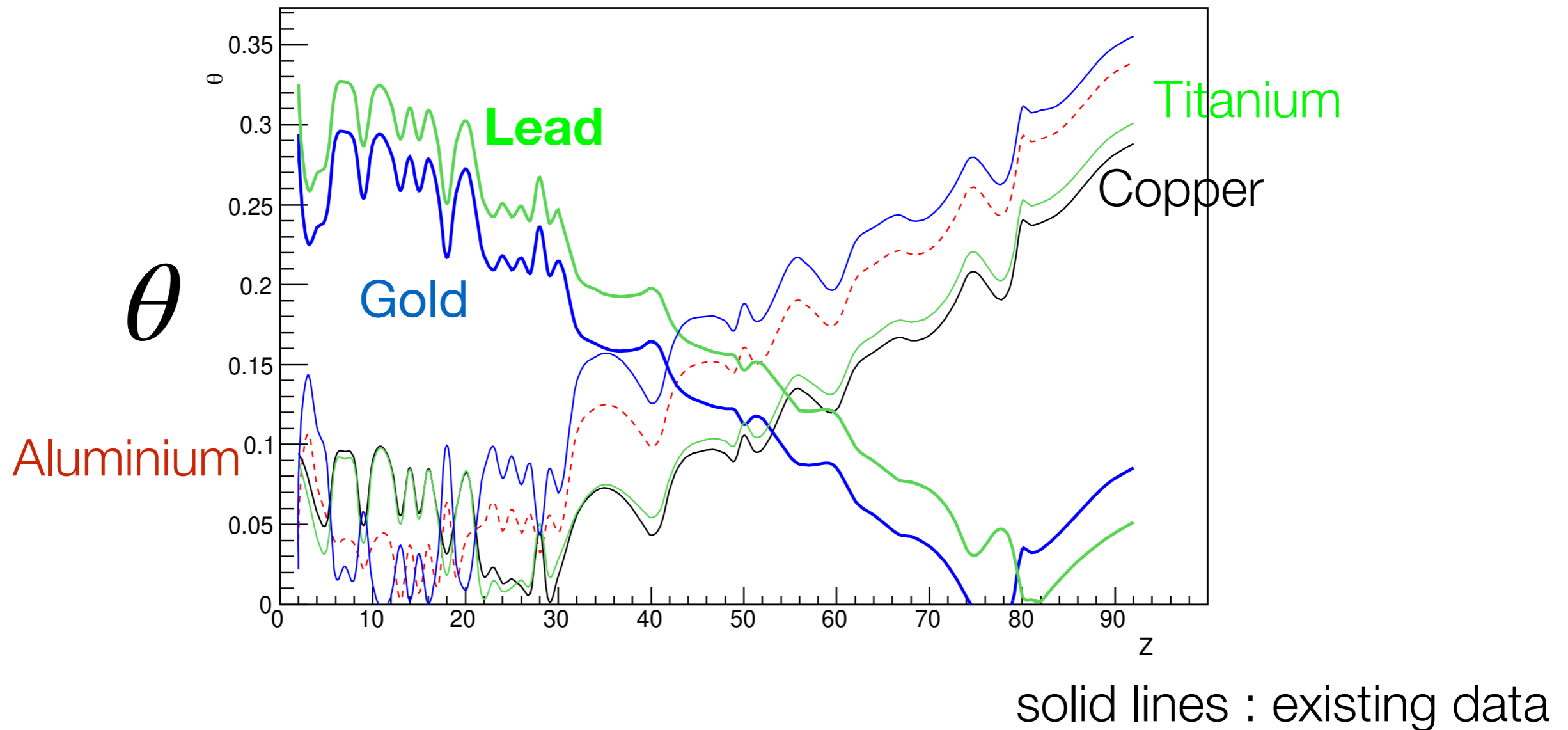


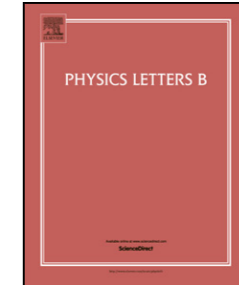
Figure 2: Angle θ between a target vector (eg dashed red = Aluminium) and other targets labelled by Z . The angle is obtained as in eqn (9), with all the dipole coefficients set to zero. The solid lines represent the targets for which there is currently data (see table 1). From smallest to largest value of θ at large Z , they are: thick green = Lead, thick blue = Gold, black = Copper, thin green = Titanium, dashed red = Aluminium, and thin blue is Sulfur. We assume that two targets can probe different coefficients if their misalignment angle is $\theta \gtrsim 0.2$ radians (or 0.1).



Contents lists available at [ScienceDirect](#)

Physics Letters B

www.elsevier.com/locate/physletb



Selecting $\mu \rightarrow e$ conversion targets to distinguish lepton flavour-changing operators



Sacha Davidson^{a,*}, Yoshitaka Kuno^b, Masato Yamanaka^c

^a LUPM, CNRS, Université Montpellier, Place Eugene Bataillon, F-34095 Montpellier, Cedex 5, France

^b Department of Physics, Osaka University, 1-1 Machikaneyama, Toyonaka, Osaka 560-0043, Japan

^c Department of Science and Technology, Kyushu Sangyo University, Fukuoka 813-8503, Japan

ARTICLE INFO

Article history:

Received 11 October 2018

Received in revised form 20 January 2019

Accepted 20 January 2019

Available online 28 January 2019

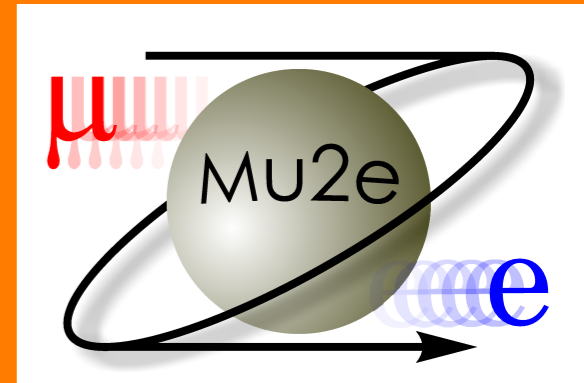
Editor: J. Hisano

ABSTRACT

The experimental sensitivity to $\mu \rightarrow e$ conversion on nuclei is set to improve by four orders of magnitude in coming years. However, various operator coefficients add coherently in the amplitude for $\mu \rightarrow e$ conversion, weighted by nucleus-dependent functions, and therefore in the event of a detection, identifying the relevant new physics scenarios could be difficult. Using a representation of the nuclear targets as vectors in coefficient space, whose components are the weighting functions, we quantify the expectation that different nuclear targets could give different constraints. We show that all but two combinations of the 10 Spin-Independent (SI) coefficients could be constrained by future measurements, but discriminating among the axial, tensor and pseudoscalar operators that contribute to the Spin-Dependent (SD) process would require dedicated nuclear calculations. We anticipate that $\mu \rightarrow e$ conversion could constrain 10 to 14 combinations of coefficients; if $\mu \rightarrow e\gamma$ and $\mu \rightarrow e\bar{e}e$ constrain eight more, that leaves 60 to 64 “flat directions” in the basis of QED \times QCD-invariant operators which describe $\mu \rightarrow e$ flavour change below m_W .

© 2019 The Author(s). Published by Elsevier B.V. This is an open access article under the CC BY license (<http://creativecommons.org/licenses/by/4.0/>). Funded by SCOAP³.

Mu2e-II - a next generation $\mu \rightarrow e$ conversion experiment at FNAL



Expression of Interest for Evolution of the Mu2e Experiment[†]

F. Abusalma²³, D. Ambrose²³, A. Artikov⁷, R. Bernstein⁸, G.C. Blazey²⁷, C. Bloise⁹, S. Boi³³, T. Bolton¹⁴, J. Bono⁸, R. Bonventre¹⁶, D. Bowring⁸, D. Brown¹⁶, D. Brown²⁰, K. Byrum¹, M. Campbell²², J.-F. Caron¹², F. Cervelli³⁰, D. Chokheli⁷, K. Ciampa²³, R. Ciolini³⁰, R. Coleman⁸, D. Cronin-Hennessy²³, R. Culbertson⁸, M.A. Cummings²⁵, A. Daniel¹², Y. Davydov⁷, S. Demers³⁵, D. Denisov⁸, S. Denisov¹³, S. Di Falco³⁰, E. Diociaiuti⁹, R. Djilkibaev²⁴, S. Donati³⁰, R. Donghia⁹, G. Drake¹, E.C. Dukes³³, B. Echenard⁵, A. Edmonds¹⁶, R. Ehrlich³³, V. Evdokimov¹³, P. Fabbri¹⁰, A. Ferrari¹¹, M. Frank³², A. Gaponenko⁸, C. Gatto²⁶, Z. Giorgio¹⁷, S. Giovannella⁹, V. Giusti³⁰, H. Glass⁸, D. Glenzinski⁸, L. Goodenough¹, C. Group³³, F. Happacher⁹, L. Harkness-Brennan¹⁹, D. Hedlin²⁷, K. Heller²³, D. Hitlin⁵, A. Hocker⁸, R. Hooper¹⁸, G. Horton-Smith¹⁴, C. Hu⁵, P.Q. Hung³³, E. Hungerford¹², M. Jenkins³², M. Jones³¹, M. Kargiantoulakis⁸, K. S. Khaw³⁴, B. Kiburgh⁸, Y. Kolomensky^{3,16}, J. Kozminski¹⁸, R. Kutschke⁸, M. Lancaster¹⁵, D. Lin⁵, I. Logashenko²⁹, V. Lombardo⁸, A. Luca⁸, G. Lukicov¹⁵, K. Lynch⁶, M. Martini²¹, A. Mazzacane⁸, J. Miller², S. Miscetti⁹, L. Morescalchi³⁰, J. Mott², S. E. Mueller¹¹, P. Murat⁸, V. Nagaslaev⁸, D. Neuffer⁸, Y. Oksuzian³³, D. Pasciuto³⁰, E. Pedreschi³⁰, G. Pezzullo³⁵, A. Pla-Dalmau⁸, B. Pollack²⁸, A. Popov¹³, J. Popp⁶, F. Porter⁵, E. Prebys⁴, V. Pronskikh⁸, D. Pushka⁸, J. Quirk², G. Rakness⁸, R. Ray⁸, M. Ricci²¹, M. Röhrken⁵, V. Rusu⁸, A. Saputi⁹, I. Sarra²¹, M. Schmitt²⁸, F. Spinella³⁰, D. Stratakis⁸, T. Strauss⁸, R. Talaga¹, V. Tereshchenko⁷, N. Tran², R. Tschirhart⁸, Z. Usbov⁷, M. Velasco²⁸, R. Wagner¹, Y. Wang², S. Werkema⁸, J. Whitmore⁸, P. Winter¹, L. Xia¹, L. Zhang⁵, R.-Y. Zhu⁵, V. Zutshi²⁷, R. Zwaska⁸

06 February 2018

Abstract

We propose an evolution of the Mu2e experiment, called Mu2e-II, that would leverage advances in detector technology and utilize the increased proton intensity provided by the Fermilab PIP-II upgrade to improve the sensitivity for neutrinoless muon-to-electron conversion by one order of magnitude beyond the Mu2e experiment, providing the deepest probe of charged lepton flavor violation in the foreseeable future. Mu2e-II will use as much of the Mu2e infrastructure as possible, providing, where required, improvements to the Mu2e apparatus to accommodate the increased beam intensity and cope with the accompanying increase in backgrounds.

Mu2e-II is an upgrade that will:

- Use ~100 kW of PIP-II protons @800 MeV
- Achieve an order of magnitude improvement in sensitivity
 - probe $R_{\mu e} \sim 10^{-18}$ level,
 - extend Λ_{NP} reach by x2



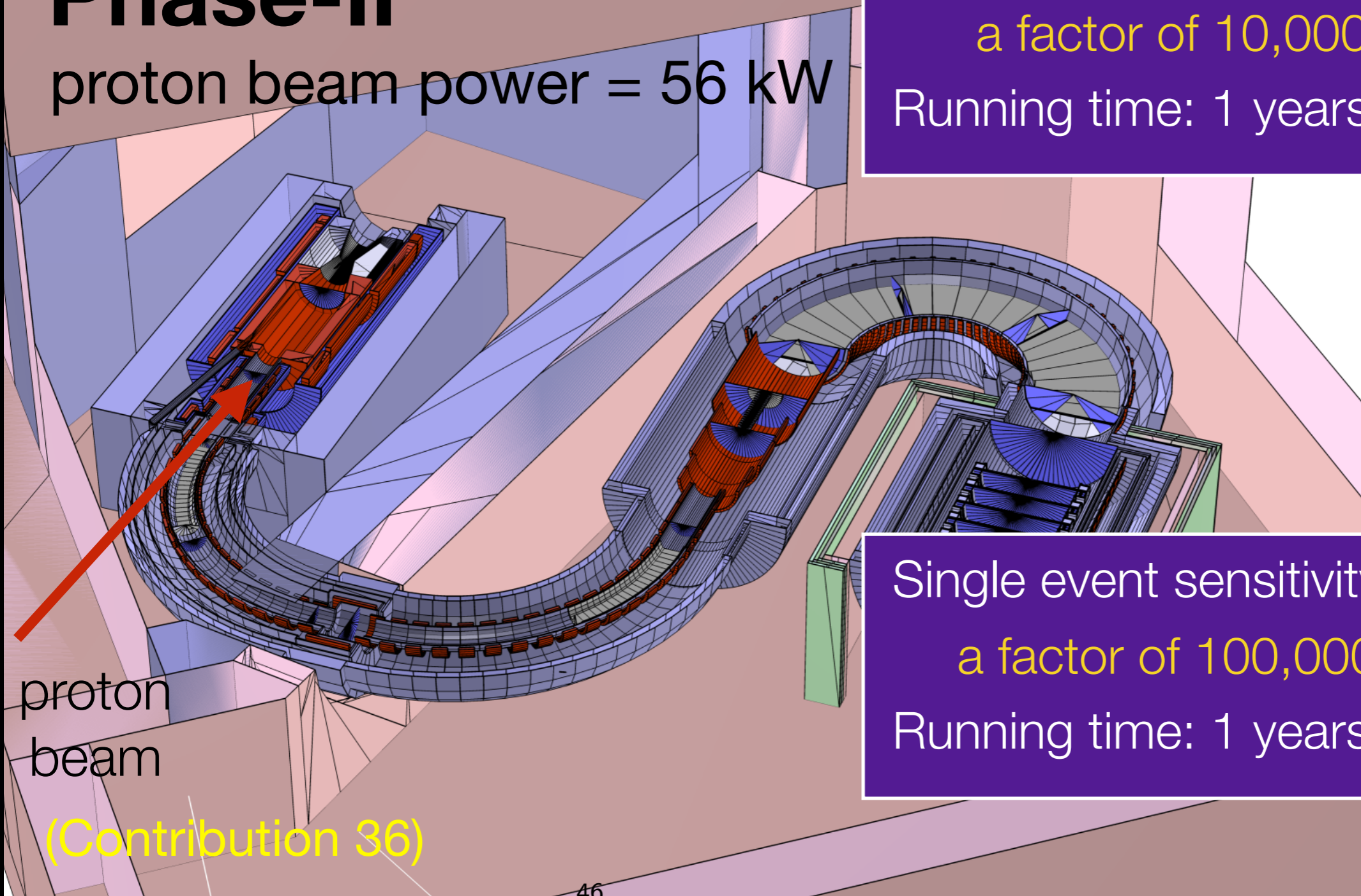
- EOI Submitted to Fermilab PAC in 2018
- arXiv:1802.02599, Fermilab-FN-1052
- 130 Signatories, 36 Institutions

PAC: “physics case is compelling” “endorse request for R&D funding”
 Status: Pursuing high priority R&D. Data taking ~2030 timescale.

COMET Phase-II : J-PARC E21

Phase-II

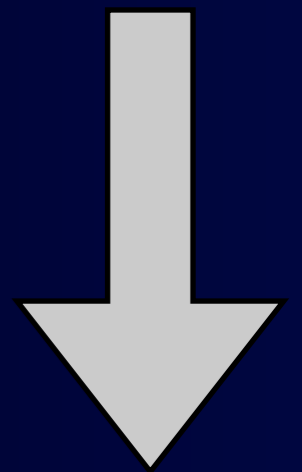
proton beam power = 56 kW



proton
beam

(Contribution 36)

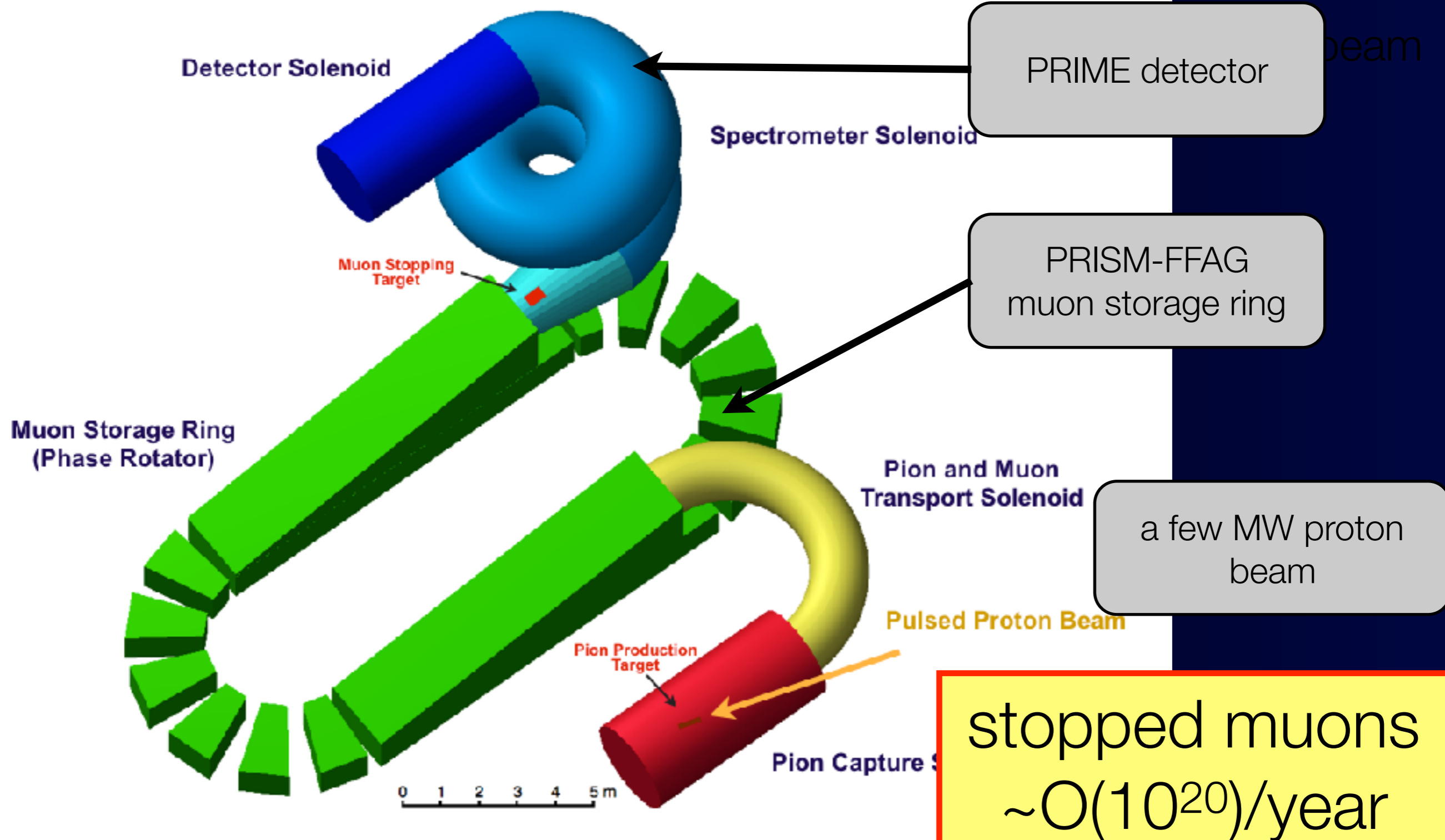
Single event sensitivity : 2.6×10^{-17}
a factor of 10,000 improvement
Running time: 1 years (2×10^7 sec)



Single event sensitivity : $O(10^{-18})$
a factor of 100,000 improvement
Running time: 1 years (3×10^7 sec)

PRISM (=Phase Rotated Intense Slow Muon source)

PRISM/PRIME



CLFV Processes

- $\mu^+ \rightarrow e^+ \gamma$
- $\mu^+ \rightarrow e^+ e^+ e^-$
- $\mu^- + N(A, Z) \rightarrow e^- + N(A, Z)$
- $\mu^- + N(A, Z) \rightarrow e^+ + N(A, Z - 2)$
- $\mu^- + N(A, Z) \rightarrow \mu^+ + N(A, Z - 2)$
- $\mu^+ e^- \rightarrow \mu^- e^+$
- $\mu^- e^- \rightarrow e^- e^-$
- $\mu + N \rightarrow \tau + X$
- $\nu_\mu + N \rightarrow \tau^+ + X$

μ^- to e^+ conversion in muonic atom



Lepton number violation (LNV) and
Lepton flavour violation (LFV)

Final can be the ground or excited states.

signal signature

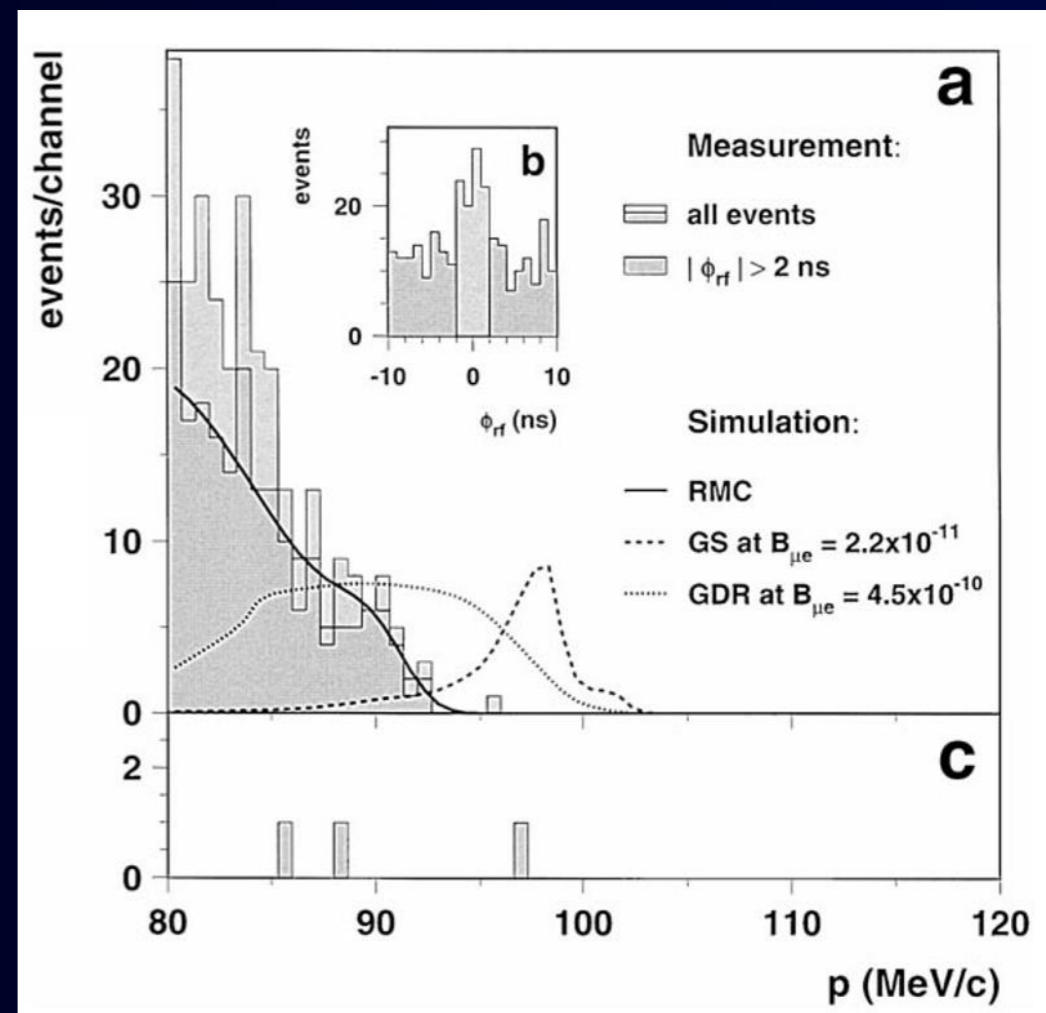
$$E_{\mu e^+} = m_\mu - B_\mu - E_{rec} - (M(A, Z - 2) - M(A, Z))$$

backgrounds

- radiative muon nuclear capture (RMC)



$$E_{RMC} = m_\mu - B_\mu - E_{rec} - (M(A, Z - 1) - M(A, Z))$$



J. Kaulard et al. (SINDRUM-II)
Phys. Lett. B422 (1998) 334.

μ^- to e^+ conversion : Target Selection



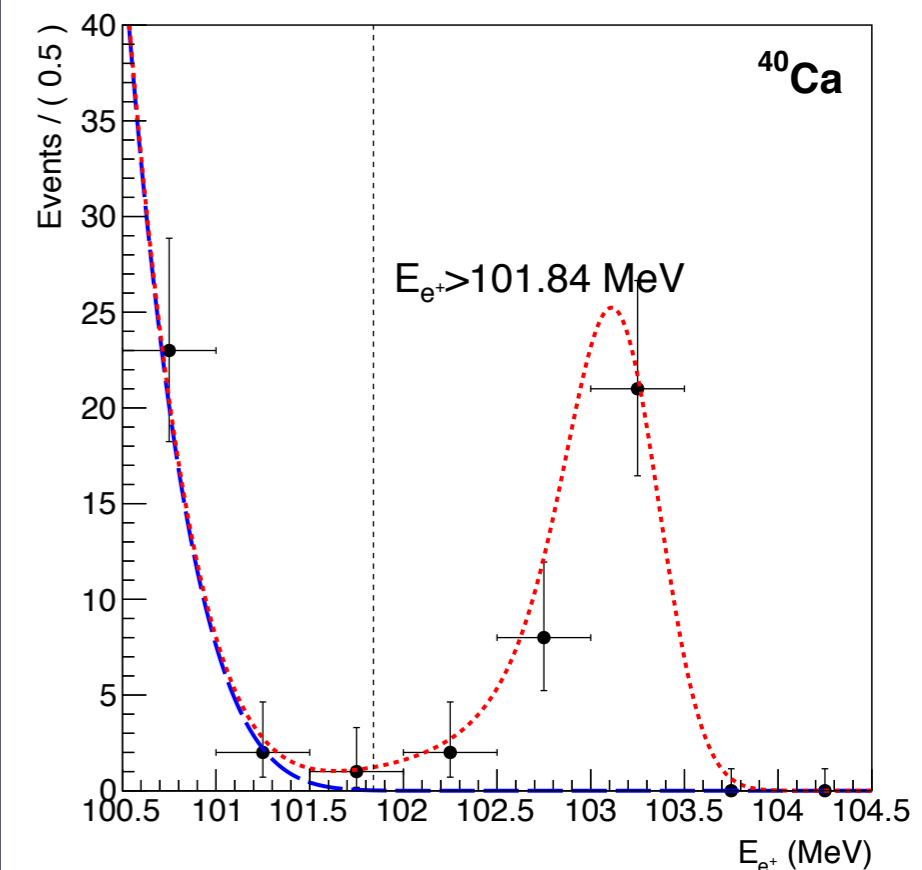
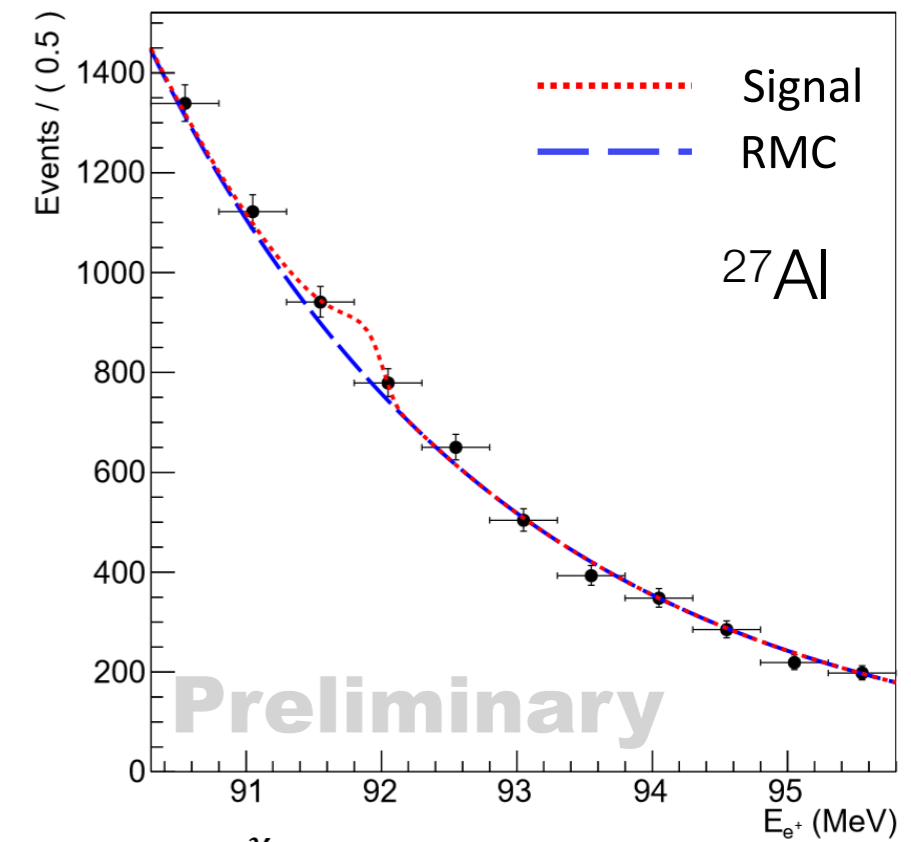
Requirement on targets

$$E_{\mu e^+} > E_{RMC} \longrightarrow M(A, Z - 1) < M(A, Z - 2)$$

Atom	$E_{\mu^- e^+}$ (MeV)	$E_{\mu^- e^-}$ (MeV)	E_{RMC}^{end} (MeV)	N.A. (%)	f_{cap} (%)	τ_{μ^-} (ns)	A_T
^{27}Al	92.30	104.97	101.34	100	61.0	864	0.191
^{32}S	101.80	104.76	102.03	95.0	75.0	555	0.142
^{40}Ca	103.55	104.39	102.06	96.9	85.1	333	0.078
^{48}Ti	98.89	104.18	99.17	73.7	85.3	329	0.076
^{50}Cr	104.06	103.92	101.86	4.4	89.4	234	0.038
^{54}Fe	103.30	103.65	101.93	5.9	90.9	206	0.027
^{58}Ni	104.25	103.36	101.95	68.1	93.1	152	0.009
^{64}Zn	103.10	103.04	101.43	48.3	93.0	159	0.011
^{70}Ge	100.67	102.70	100.02	20.8	92.7	167	0.013

Aluminum (for COMET & Mu2e) is not good.

10^{18} muons, signal $\sim 1 \times 10^{-12}$



CLFV of
Muon Bound States



CLFV Processes

- $\mu^+ \rightarrow e^+ \gamma$
- $\mu^+ \rightarrow e^+ e^+ e^-$
- $\mu^- + N(A, Z) \rightarrow e^- + N(A, Z)$
- $\mu^- + N(A, Z) \rightarrow e^+ + N(A, Z - 2)$
- $\mu^- + N(A, Z) \rightarrow \mu^+ + N(A, Z - 2)$
- $\mu^+ e^- \rightarrow \mu^- e^+$
- $\mu^- e^- \rightarrow e^- e^-$
- $\mu + N \rightarrow \tau + X$
- $\nu_\mu + N \rightarrow \tau^+ + X$

Muonium to Antimuonium Conversion

Mu (μ^+e^-) \rightarrow anti-Mu (μ^-e^+)



$$|\Delta L_{\mu/e}| = 2$$

- models : doubly-charged Higgs etc.
- muonium production in vacuum
 - SiO₂ powder
- antimuonium detection
 - high energy e⁻ in $\mu^- \rightarrow e^- \nu \bar{\nu}$
 - low energy e⁺ annihilation

- effective theory with contact interaction

$$\delta \equiv 2 \langle \bar{M} | H_{\text{Mu}\bar{\text{Mu}}} | M \rangle = \frac{8 G_F}{\sqrt{2} n^2 \pi a_0^3} \left(\frac{G_{\text{Mu}\bar{\text{Mu}}}}{G_F} \right)$$

- for ground state

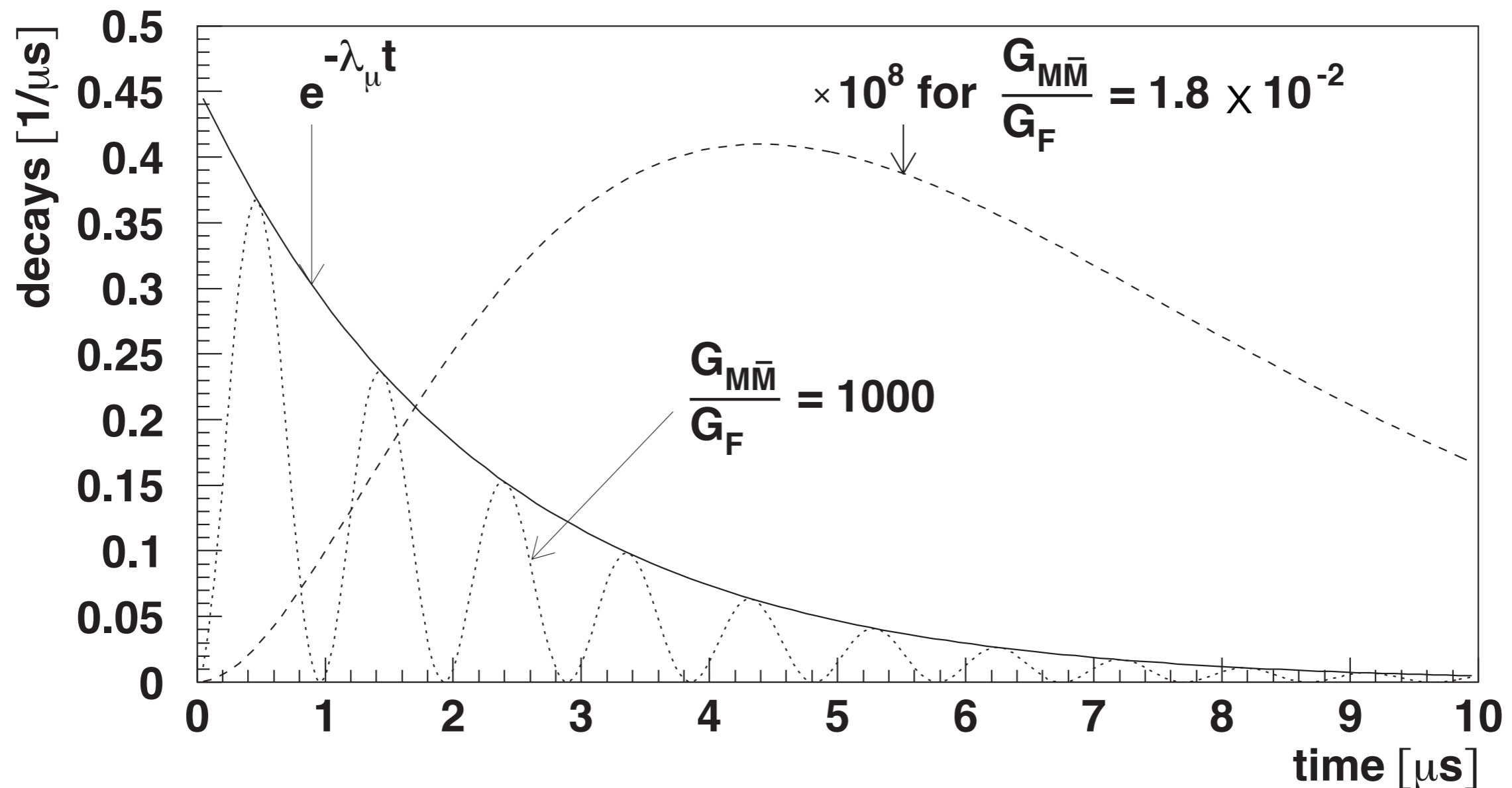
$$\delta = 1.5 \times 10^{-12} \cdot \left(\frac{G_{\text{Mu}\bar{\text{Mu}}}}{G_F} \right) \quad (\text{eV})$$

- oscillation probability

$$p_{\text{Mu}\bar{\text{Mu}}}(t) = \sin^2 \left(\frac{\delta t}{2} \right) \cdot \lambda_\mu e^{-\lambda_\mu t} \approx \left(\frac{\delta t}{2} \right)^2 \cdot \lambda_\mu e^{-\lambda_\mu t}$$

Muonium to Antimuonium Conversion

Mu (μ^+e^-) \rightarrow anti-Mu (μ^-e^+)



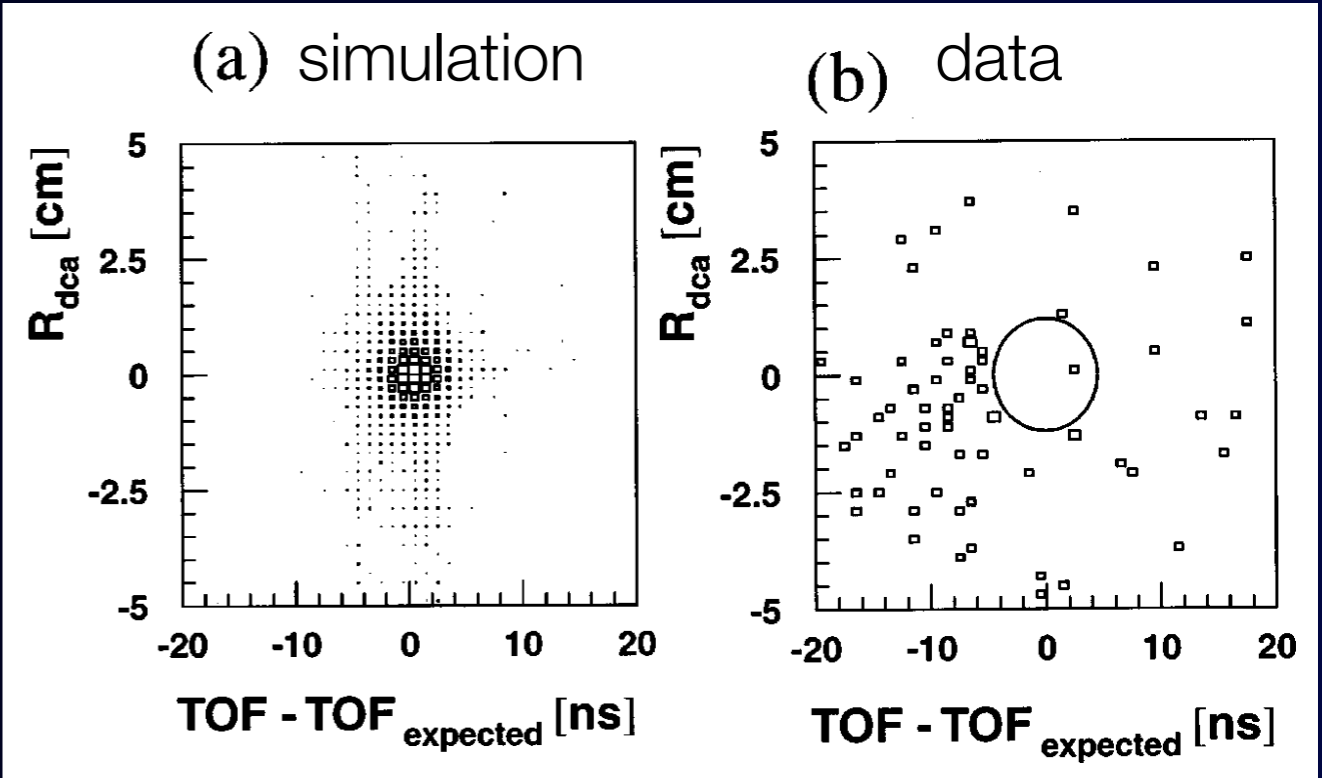
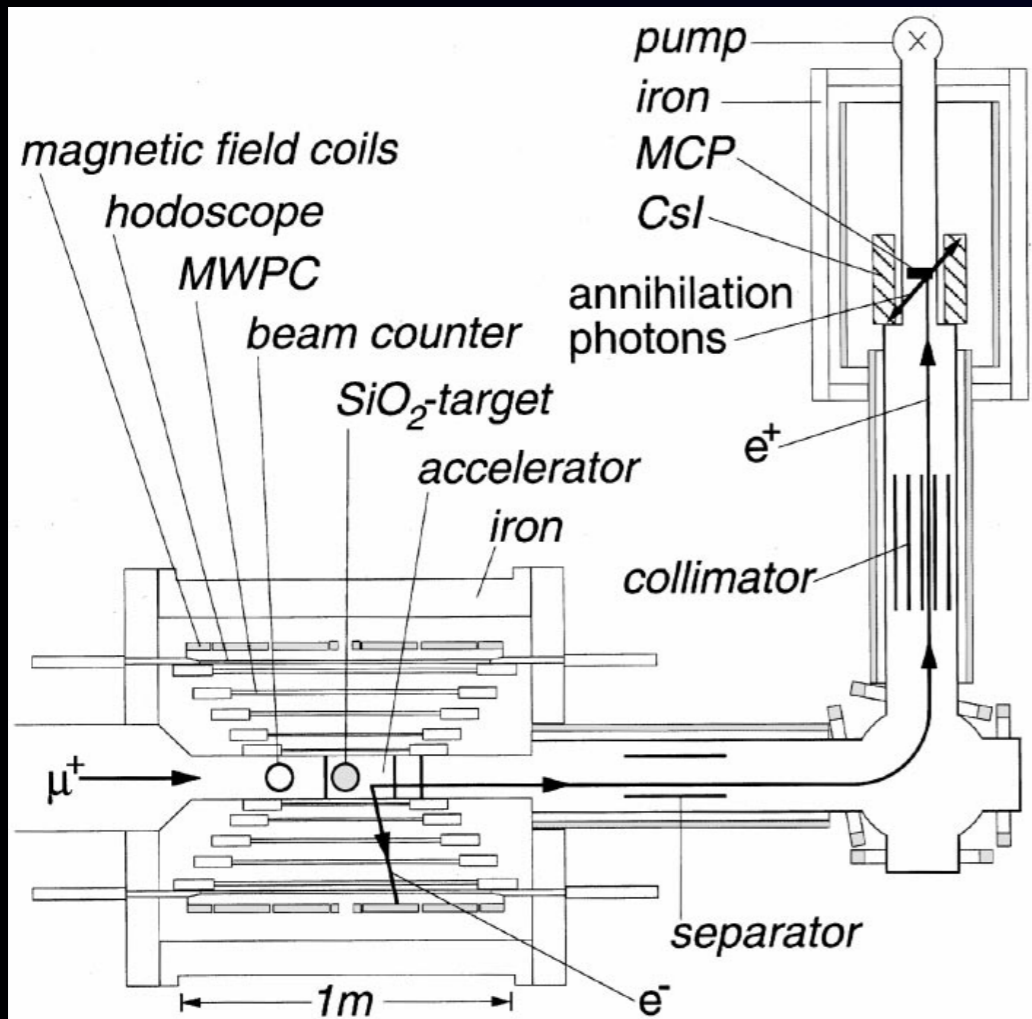
Muonium to Antimuonium Conversion

$\text{Mu} (\mu^+e^-) \rightarrow \text{anti-Mu} (\mu^-e^+)$

$$\mu^+ + e^- \rightarrow \mu^- + e^+$$

Previous experiment

SINDRUM experiment at PSI (1999)



$$G_{\text{Mu}\overline{\text{Mu}}} < 3 \times 10^{-3} G_F \quad \text{data}$$

Future prospects:

- new attempt at MUSE/J-PARC ?
 - laser ionization
- new attempt in China?
 - new accelerator

Muonium CLFV Decay

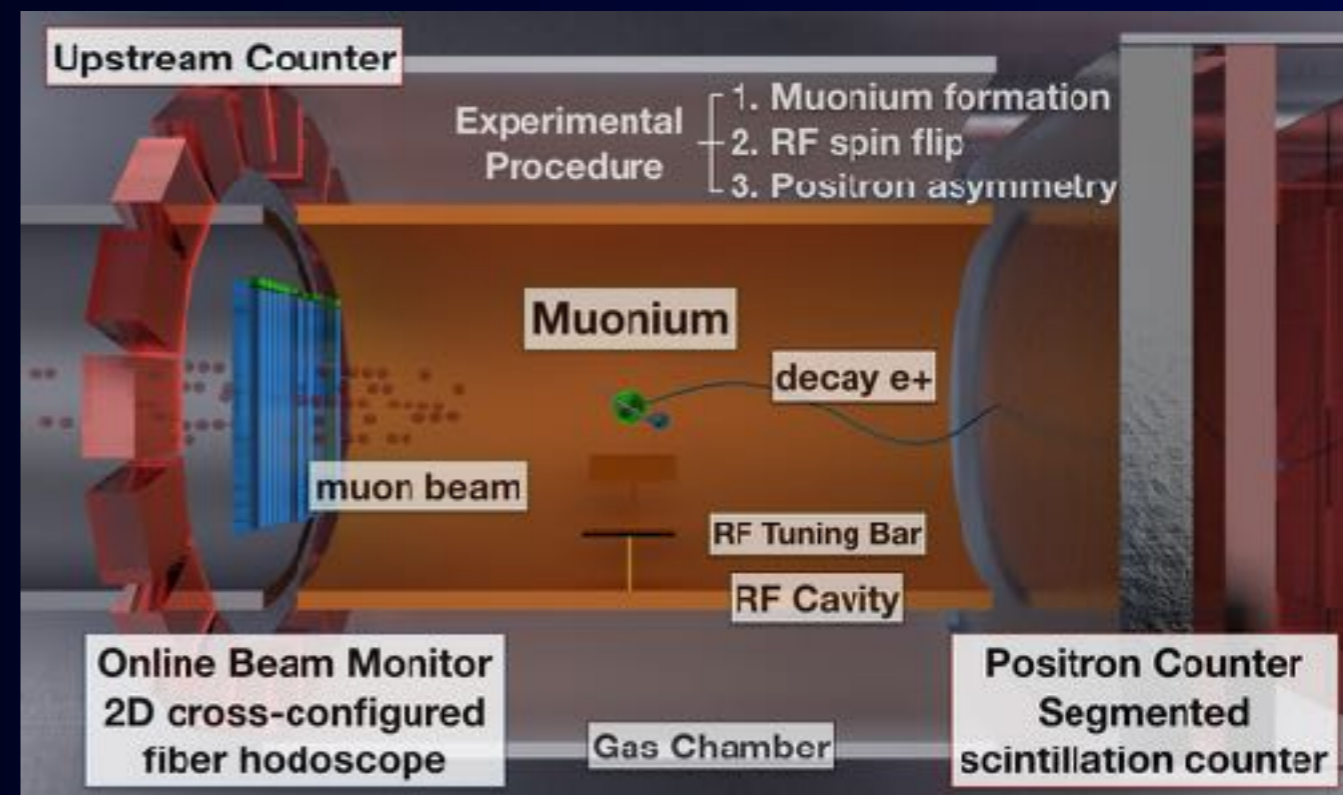


- similar to $\mu \rightarrow eee$
 - may be useful to distinguish different couplings
 - 2 body final state
- disadvantage
 - poor-wave function overlap between μ and e
 - Coulomb bound state

Museum detector
@J-PARC

Future prospects:

- no experiments so far
- muonium production in MUSEUM at MUSE @ J-PARC
 - measurement of hyperfine splitting
 - 10^{15} for 2×10^7 sec

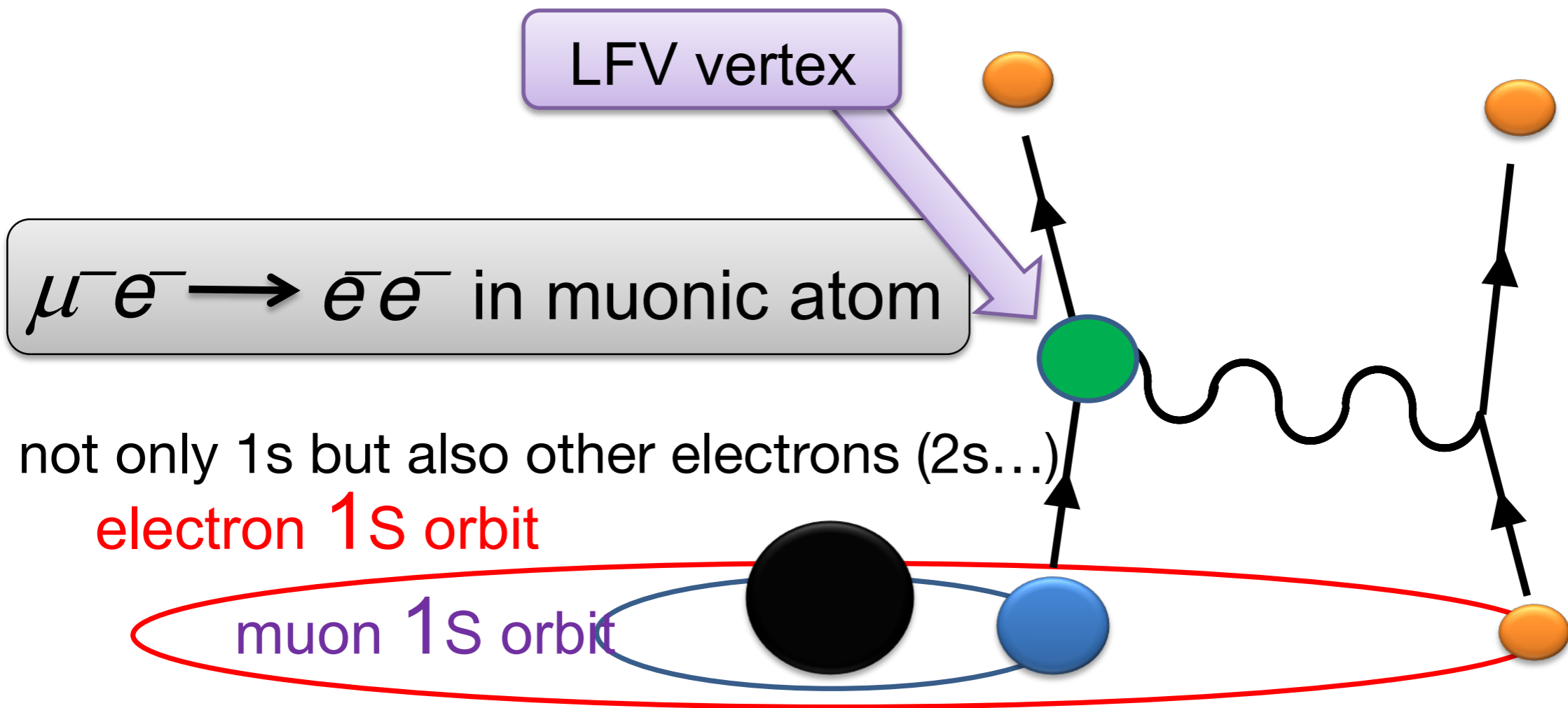


CLFV Processes

- $\mu^+ \rightarrow e^+ \gamma$
- $\mu^+ \rightarrow e^+ e^+ e^-$
- $\mu^- + N(A, Z) \rightarrow e^- + N(A, Z)$
- $\mu^- + N(A, Z) \rightarrow e^+ + N(A, Z - 2)$
- $\mu^- + N(A, Z) \rightarrow \mu^+ + N(A, Z - 2)$
- $\mu^+ e^- \rightarrow \mu^- e^+$
- $\mu^- e^- \rightarrow e^- e^-$
- $\mu + N \rightarrow \tau + X$
- $\nu_\mu + N \rightarrow \tau^+ + X$

$\mu^- + e^- \rightarrow e^- + e^-$ in a muonic atom

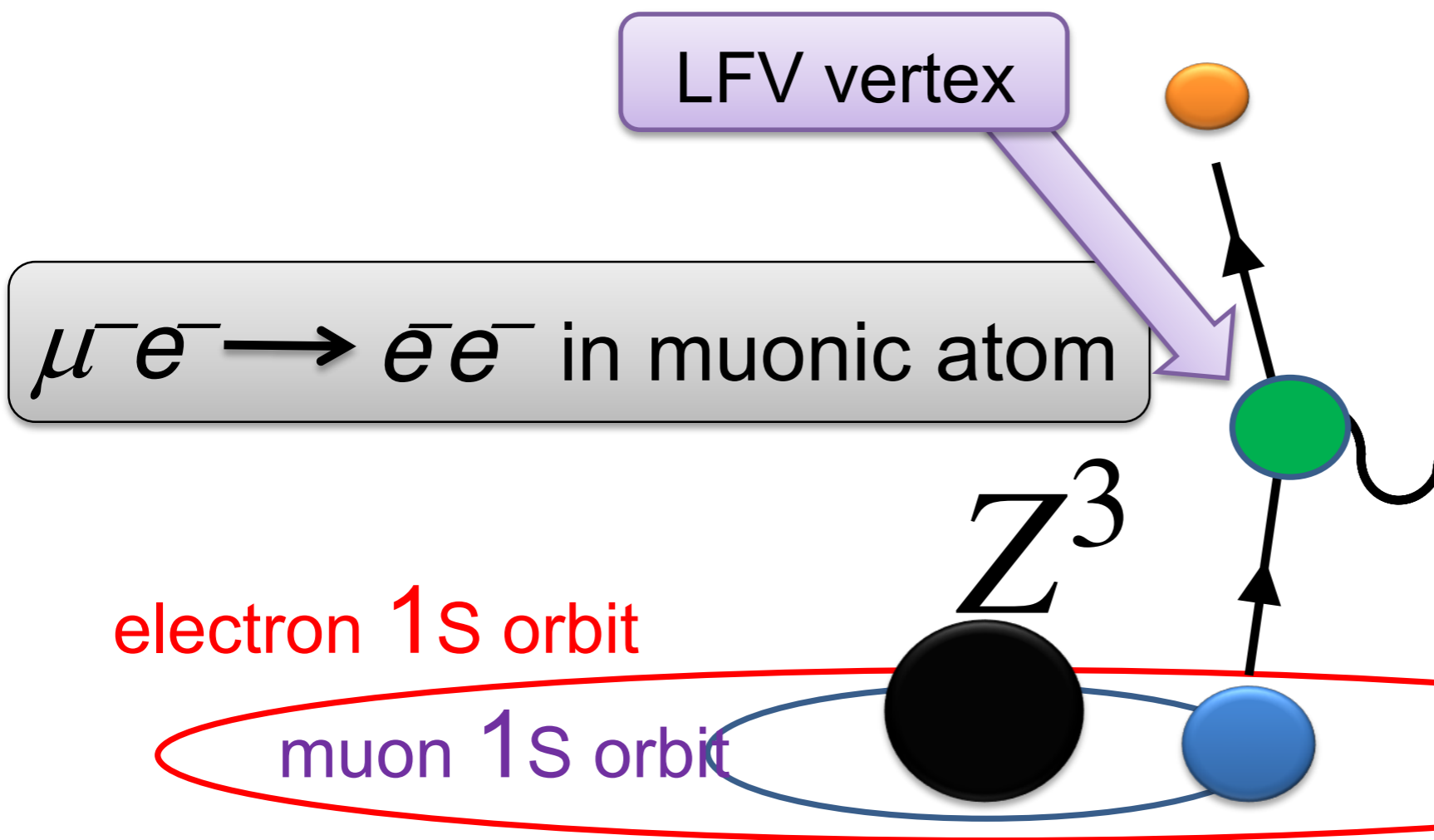
$$\mu^- + e^- \rightarrow e^- + e^-$$



- Original idea
M. Koike, YK, J. Sato and M. Yamanaka, Phys. Rev. Lett. 105 (2010)

$\mu^- + e^- \rightarrow e^- + e^-$ in a muonic atom

$$\mu^- + e^- \rightarrow e^- + e^-$$



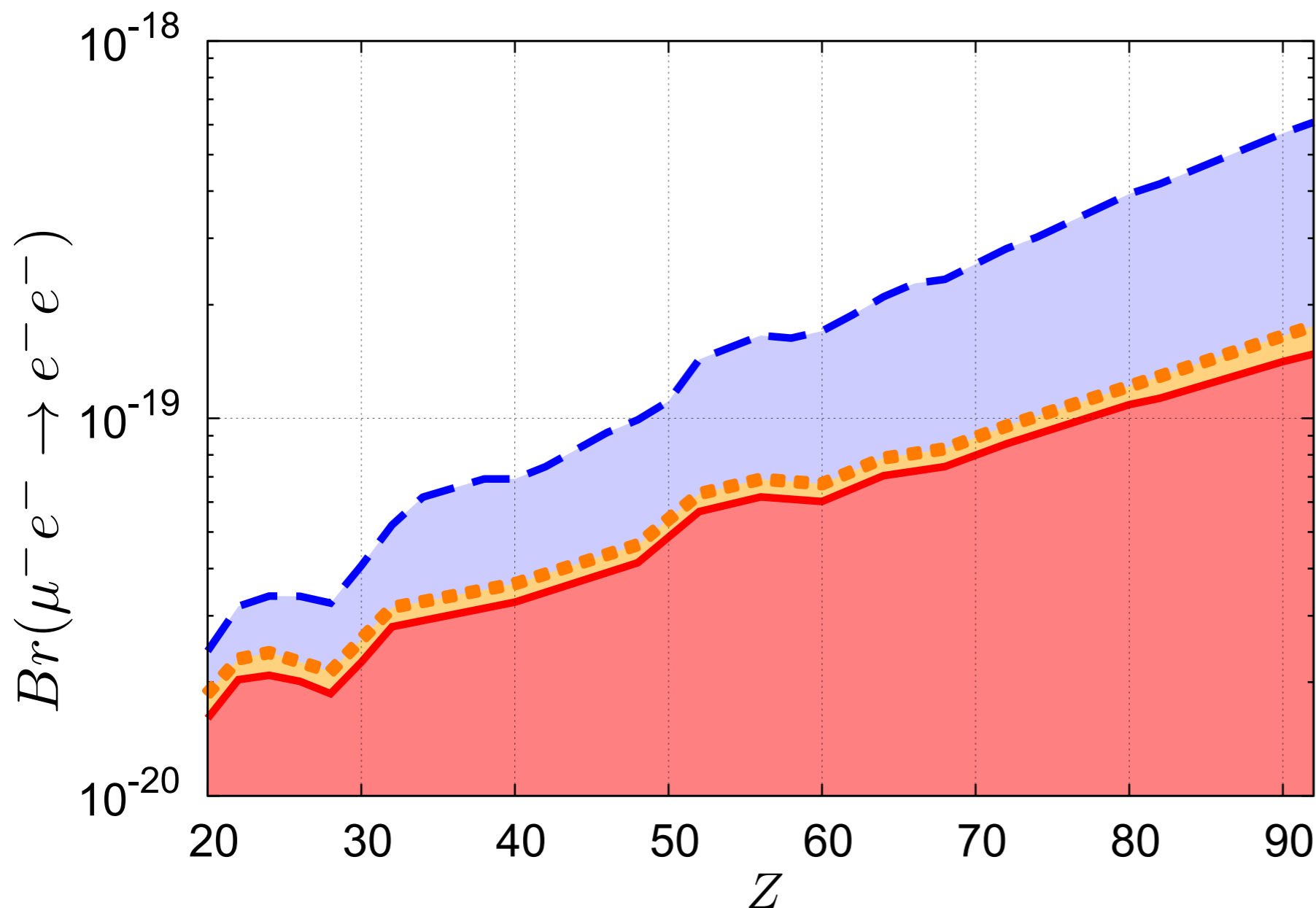
$\mu^- e^- \rightarrow e^- e^-$ has the overlap of μ^- and e^- which is proportional to Z^3 . For instance, $Z=80$, enhancement of 5×10^5 .

Experimentally measurement of a pair of e^- and e^- in the final state is easier (larger phase space).

- Original idea
M. Koike, YK, J. Sato and M. Yamanaka, Phys. Rev. Lett. 105 (2010)

$\mu^- + e^- \rightarrow e^- + e^-$ in a muonic atom

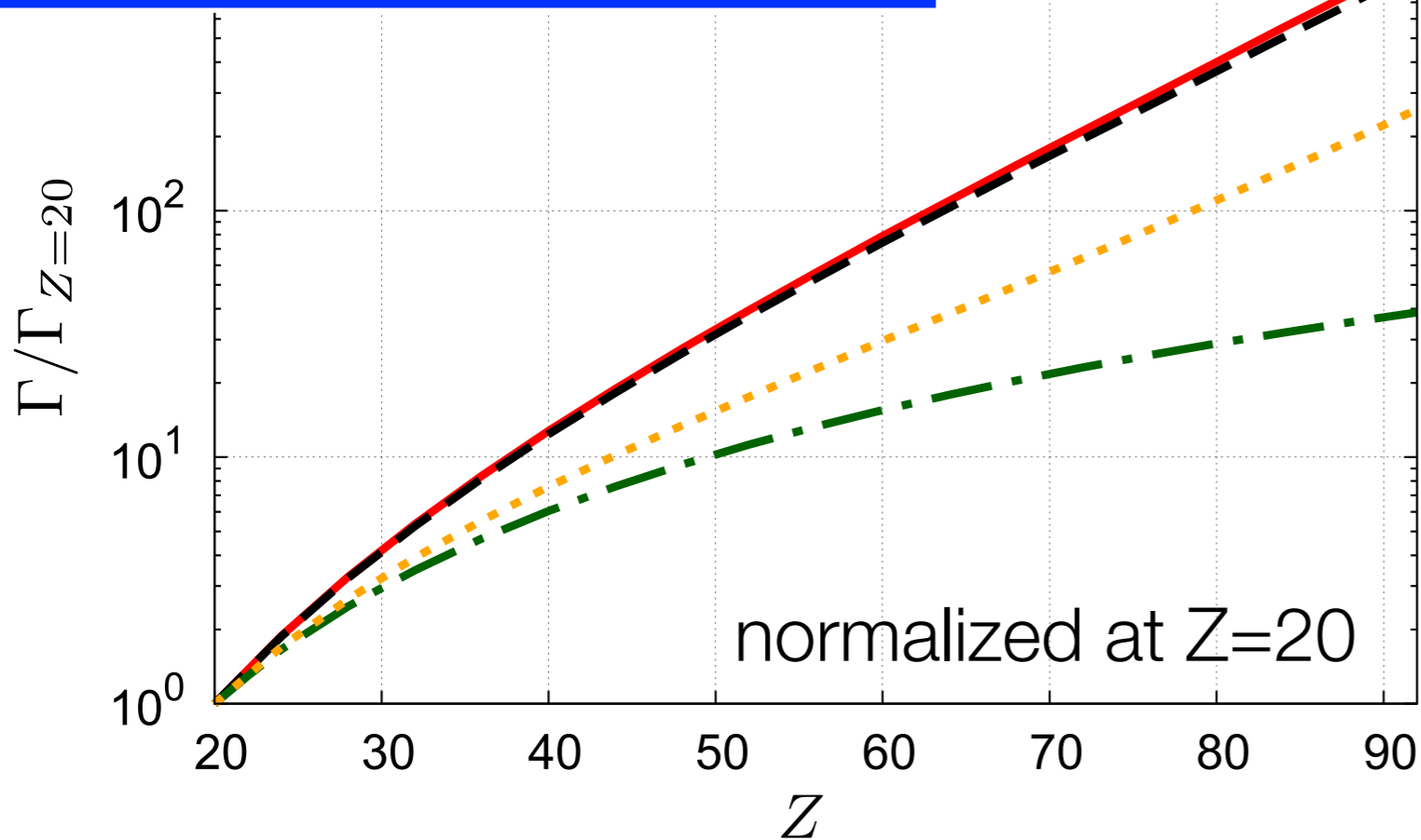
$$\mu^- + e^- \rightarrow e^- + e^-$$



upper limits
from the current
 $\mu^- \rightarrow e^- + e^- + e^-$

why are we
interested in ?

$\mu^- + e^- \rightarrow e^- + e^-$ in a muonic atom : Z dependence for model discrimination



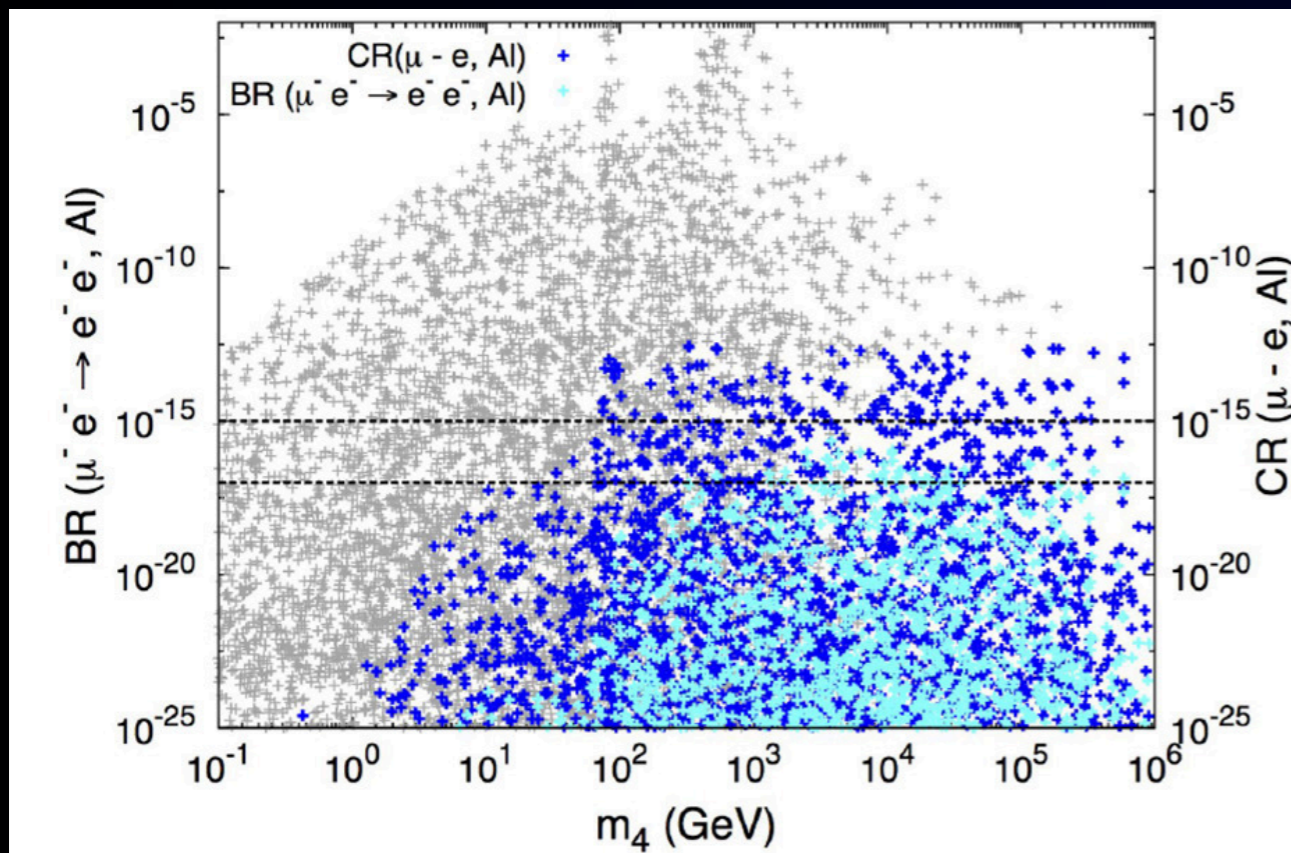
- (1) solid red line : contact int. with the same chirality
- (2) a dashed black line : contact int. with opposite chirality
- (3) a dash-dotted green line : photonic int.
- (4) a dotted orange line : mix of contact and photonic int.

- Study of contact interaction with different Z targets
Y. Uesaka, YK, J. Sato, T. Sato and M. Yamanaka, Phys. Rev. D93 (2016) 076006
- Study of long-distance dipole interaction with different Z targets
Y. Uesaka, YK, J. Sato, T. Sato and M. Yamanaka, Phys. Rev. D97 (2018) 015017

Heavy Neutral Lepton (HNL) Models for $\mu^- + e^- \rightarrow e^- + e^-$ in a muonic atom



(3+1) model

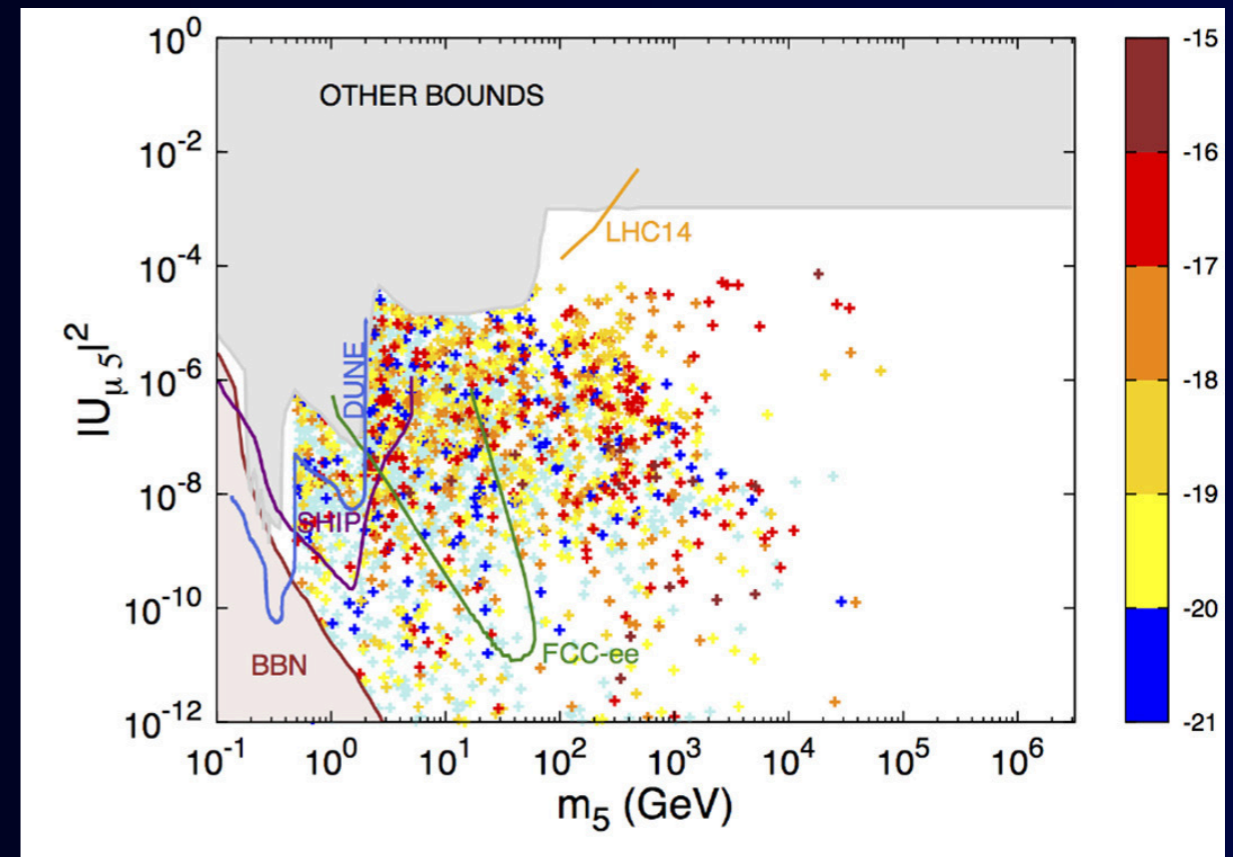


m_4 : HNL mass

cyan points : $\mu^- + e^- \rightarrow e^- + e^-$

blue points : $\mu^- + \text{Al} \rightarrow e^- + \text{Al}$

(3+2) model



m_5 : HNL mass

colored points : $\text{Br}(\mu^- + e^- \rightarrow e^- + e^-)$

CLFV Processes

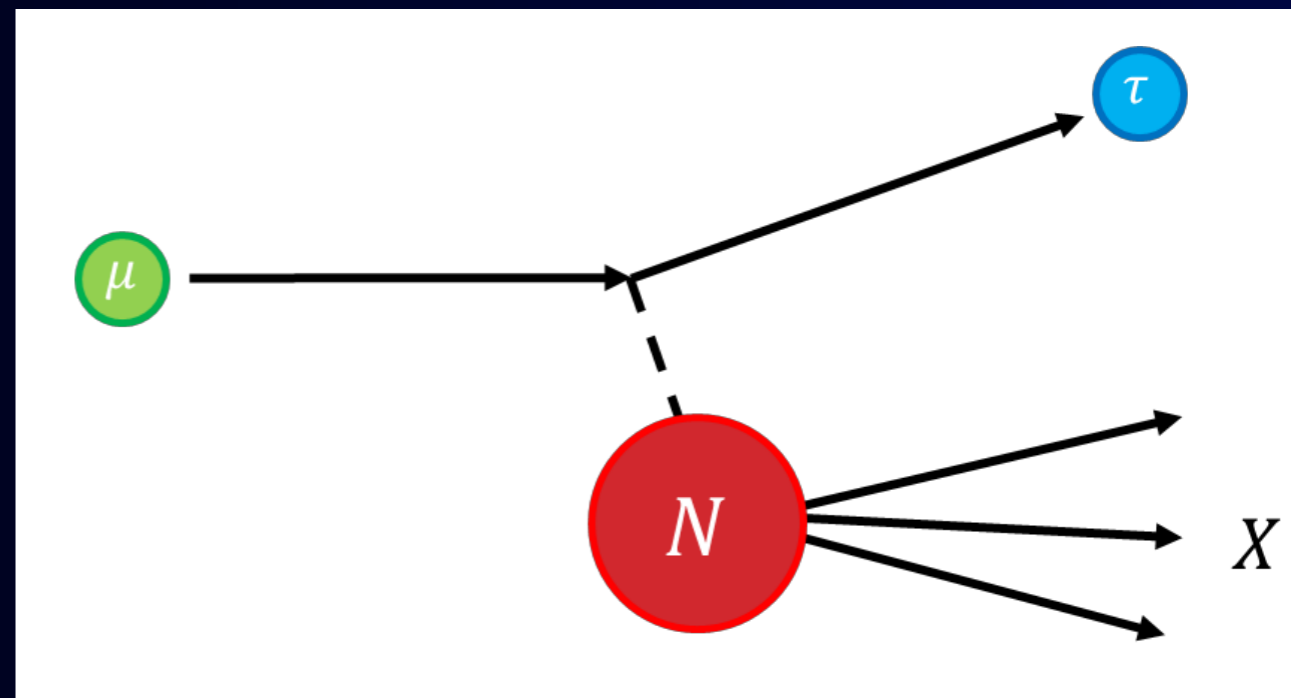
- $\mu^+ \rightarrow e^+ \gamma$
 - $\mu^+ \rightarrow e^+ e^+ e^-$
 - $\mu^- + N(A, Z) \rightarrow e^- + N(A, Z)$
 - $\mu^- + N(A, Z) \rightarrow e^+ + N(A, Z - 2)$
 - $\mu^- + N(A, Z) \rightarrow \mu^+ + N(A, Z - 2)$
 - $\mu^+ e^- \rightarrow \mu^- e^+$
 - $\mu^- e^- \rightarrow e^- e^-$
- $\mu + N \rightarrow \tau + X$
- $\nu_\mu + N \rightarrow \tau^+ + X$

CLFV Scattering Process

$$\mu + N (e + N) \rightarrow \tau + X$$

$$m_{\mu} < m_{\tau}$$

inelastic scattering (DIS) region with high-intensity and high-energy muon (electron) beams



- the search with scattering is less effective than searches with decays (weak interaction cross section $\sim 10^{-45}$ barns at 1MeV)
- scattering cross section increases as incident energy is higher.
- electron beam from ILC (at beam dump) or muon beam from muon collider can be considered.

M. Sher and I. Turan, Phys. Rev. D 69, 017302 (2004).

S. Kanemura, YK, M. Kuze and T. Ota, Phys. Lett. B607 (2005) 165

M. Takeuchi, Y. Uesaka, M. Yamanaka, Phys. Lett. B772 (2017) 279

CLFV Scattering Process

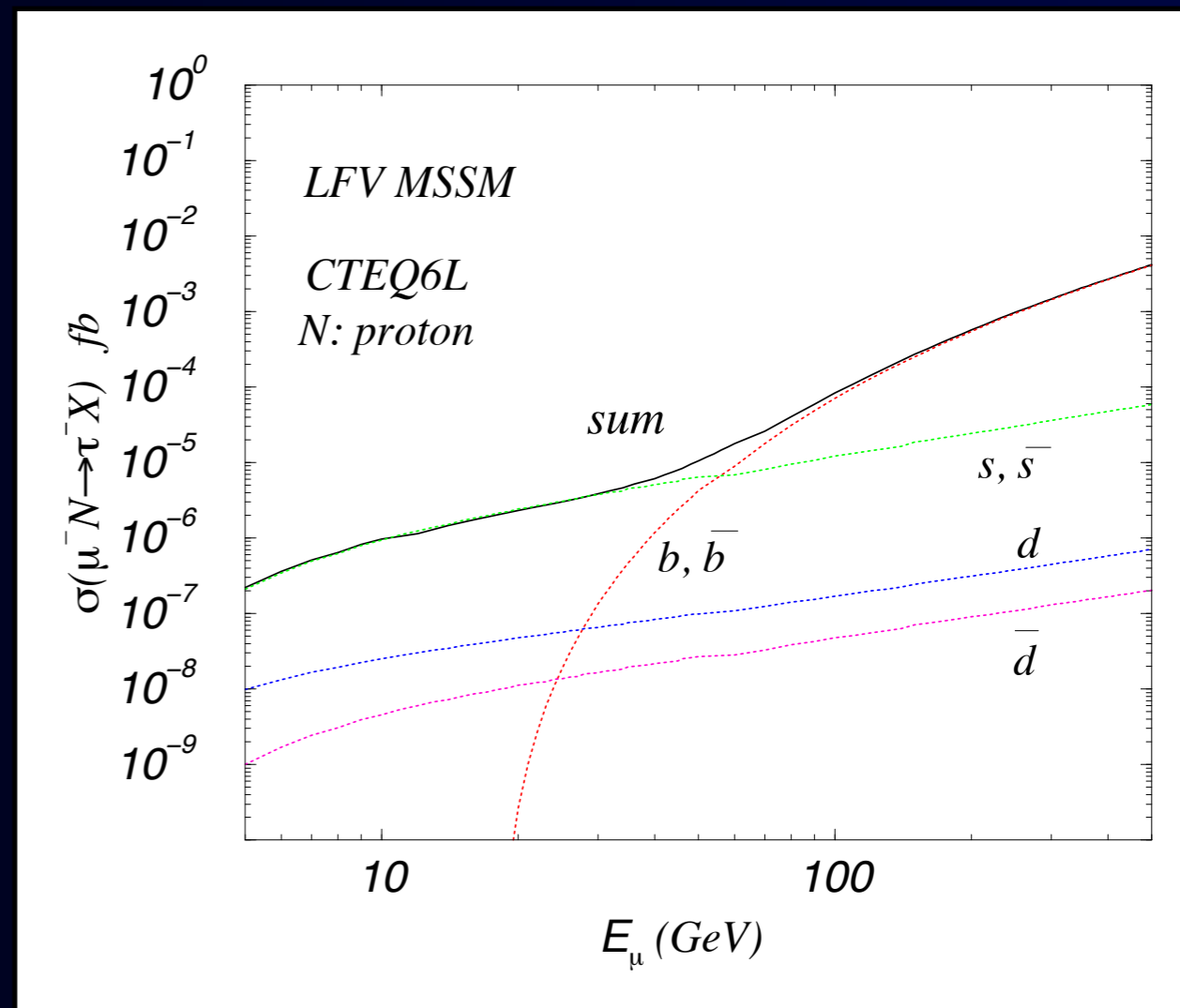
$$\mu + N (e + N) \rightarrow \tau + X$$

Minimum supersymmetric model (MSSM) with Higgs mediated LFV coupling

Upper limits from tau decays is given.

$$\tau \rightarrow \mu\eta$$

$\sigma < 10^{-5}$ fb for 50 GeV muons.



M. Sher and I. Turan, Phys. Rev. D 69, 017302 (2004).

S. Kanemura, YK, M. Kuze and T. Ota, Phys. Lett. B607 (2005) 165

M. Takeuchi, Y. Uesaka, M. Yamanaka, Phys. Lett. B772 (2017) 279

CLFV Processes

- $\mu^+ \rightarrow e^+ \gamma$
- $\mu^+ \rightarrow e^+ e^+ e^-$
- $\mu^- + N(A, Z) \rightarrow e^- + N(A, Z)$
- $\mu^- + N(A, Z) \rightarrow e^+ + N(A, Z - 2)$
- $\mu^- + N(A, Z) \rightarrow \mu^+ + N(A, Z - 2)$
- $\mu^+ e^- \rightarrow \mu^- e^+$
- $\mu^- e^- \rightarrow e^- e^-$
- $\mu + N \rightarrow \tau + X$
- $\nu_\mu + N \rightarrow \tau^+ + X$

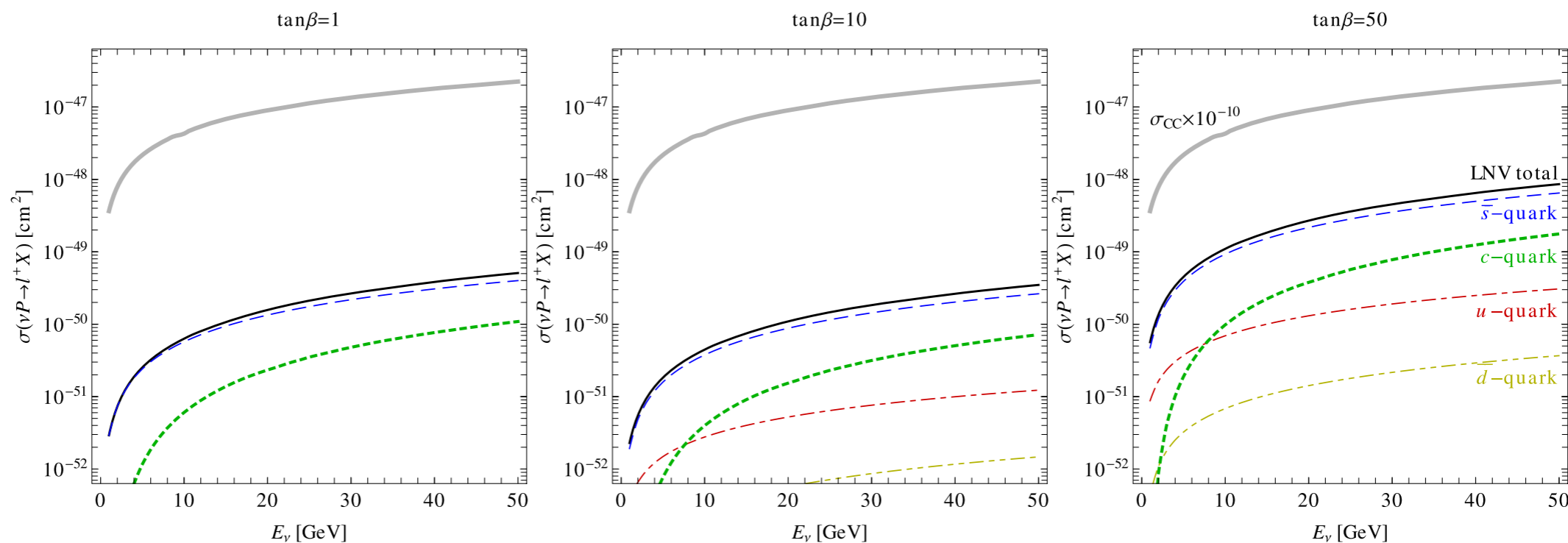
LNV Charged Current Scattering Process



LNV LFV charged current (LNV-CC) interaction

- measurement can be made at a neutrino near detector with a magnetic field to identify an electric charge of the charged leptons
- at production like $\pi^+ \rightarrow \mu^+ \bar{\nu}_\alpha$
- at detector

10^{-48}cm^2
at 50 GeV



Summary

- CLFV processes provide a unique discovery potential for physics beyond the Standard Model (BSM), exploring new physics parameter space in a manner complementary to the collider, dark matter, dark energy, and neutrino physics programs.
- CLFV experimental programs are rich, being covered by low energy to high energy measurements.
- In particular, the muon CLFV programs are expecting significant progress owing to improvement of the muon sources in coming years.



Thank you!

谢谢

ありがとう!

